DOI:10.1093/jnci/djs377
Advance Access publication on September 13, 2012.

ARTICLE

Protumorigenic Activity of Plasminogen Activator Inhibitor-1 Through an Antiapoptotic Function

Hua Fang, Veronica R. Placencio, Yves A. DeClerck

Manuscript received November 10, 2011; revised July 20, 2012; accepted July 24, 2012.

Correspondence to: Yves A. DeClerck, MD, Division of Hematology-Oncology, Children's Hospital Los Angeles, MS #54, 4650W Sunset Blvd, Los Angeles, CA 90027 (e-mail: declerck@usc.edu).

Background Plasminogen activator inhibitor-1 (PAI-1) is a protease inhibitor but is paradoxically associated with poor outcomes in cancer patients. However, the mechanisms of its effects on tumor cells have not been explored.

Methods Endogenous PAI-1 in human tumor cell lines (HT-1080, A549, HCT-116, and MDA-MB-231) was suppressed by small interfering RNAs (siRNAs) and PAI-039, a small molecule inhibitor of PAI-1, and the effects on apoptosis were examined. Tumorigenicity of PAI-1 knockdown (KD) tumor cells was examined in immunodeficient PAI-1 wild-type and knockout (KO) mice (9–15 per group), and event-free survival was analyzed by the Kaplan–Meier method. The effect of PAI-1 suppression on HT-1080 xenotransplanted tumors was evaluated for cell proliferation, apoptosis, and angiogenesis. All statistical tests were two-sided.

Results Genetic and pharmacological inhibition of PAI-1 in the four tumor cell lines increased spontaneous apoptosis (mean fold increase relative to control: HT-1080, siRNA#1, mean = 4.0, 95% CI = 2.6 to 5.3, $P < .001$; siRNA#2, mean = 2.6, 95% CI = 2.4 to 2.9, $P < .001$, Student t test), which was blocked in the presence of recombinant PAI-1, a caspase-8 inhibitor, or Fas/FasL neutralizing antibodies and was partially attenuated by a plasmin inhibitor-aprotinin. PAI-1 KO mice implanted with PAI-1 KD HT-1080 cells had decreased tumorigenesis and prolonged survival compared with control mice ($P = .002$, log-rank test), and their tumors exhibited decreased cell proliferation and angiogenesis and increased apoptosis. Furthermore, five of 15 PAI-1 KO mice implanted with PAI-1 KD HT-1080 cells never developed tumors.

Conclusions These data suggest that PAI-1 exerts a protective effect against tumor cell apoptosis by a mechanism that, in part, involves plasmin activation and inhibition of Fas/Fas-L-mediated apoptosis and may be a promising therapeutic target.

J Natl Cancer Inst 2012;104:1470–1484

Extracellular proteases play an important regulatory role in many biological and pathological processes, such as organ development, tissue injury and repair, inflammation, and cancer (1,2). They process not only extracellular matrix proteins but also growth factors, membrane-associated receptors, a large variety of ligands, and proenzymes (3). Because of the large variety of substrates they target, extracellular proteases have a complex role in cancer and have been shown to have an antitumorigenic as well as a protumorigenic function. Adding to the complexity of their function is the fact that their activity is tightly regulated by natural inhibitors, which often have other functions besides the control of extracellular proteolysis.

Such a complex role is well illustrated in the case of the urokinase plasminogen activator (uPA)-plasmin system, which is one of the most investigated protease systems in cancer (4–6). The serine protease uPA concentrates at the cell surface where it becomes activated upon binding to its specific receptor uPAR (7); activated uPA then cleaves plasminogen into plasmin, which is a broad-spectrum serine protease that, in addition to degrading proteins such as fibrin and multiple extracellular matrix glycoproteins, activates prometalloproteases and converts progrowth factors into their active forms (6,8). Typically, these effects result in an increase in tumor cell proliferation, migration, invasion, and metastasis. Accordingly, elevated levels of uPA and uPAR expression in blood and tumor tissues have been reported to be associated with poor clinical outcome and a decreased response to chemotherapy in many different types of cancer (9–13). The proteolytic activity of uPA is specifically controlled by plasminogen activator inhibitor-1 (PAI-1), which upon binding to uPA promotes the rapid endocytosis of the trimolecular uPA/PAI-1/uPAR complex (14–16). In addition to its antiproteolytic activity, PAI-1 has an antiadhesive function on cells as it competes with uPAR and integrins for binding to vitronectin (17). It was initially thought that these two major functions of PAI-1 would support an antitumorigenic role and that elevated levels of PAI-1 in cancer would be a predictor of better outcome. Surprisingly and

paradoxically, elevated levels of PAI-1 in tumor samples and blood of cancer patients were discovered to predict a poorer rather than a favorable clinical outcome in a large variety of cancers including gastric (18), colorectal (19), breast (20,21), ovarian (22,23), and lung cancer (24), suggesting that PAI-1 positively contributes to cancer progression.

This paradoxical role of PAI-1 in cancer has been primarily attributed to its proangiogenic function in the extracellular milieu. It has been shown that in tumor-bearing PAI-1–deficient mice, there is a defect in angiogenesis (25,26), and our laboratory has previously reported that PAI-1 stimulates angiogenesis by promoting endothelial cell (EC) migration from vitronectin-rich perivascular space toward fibronectin-containing tumor tissue (27). We later demonstrated that PAI-1 protects ECs from Fas/Fas ligand (FasL)-mediated apoptosis. This latter effect was found to be the result of inhibition of plasmin-mediated cleavage of membrane-associated FasL into a proapoptotic soluble FasL fragment (28).

The complex components, uPA, uPAR, and PAI-1, are also expressed by tumor cells (29), and PAI-1 has been shown to regulate apoptosis in both normal and cancer cells (30,31), but the mechanisms have not been fully explored. Furthermore, studies have suggested that PAI-1 primarily acts extracellularly. This leaves the question of whether stroma-derived PAI-1 could compensate for a lack of PAI-1 in tumor cells and vice versa. Here we have examined the effect of PAI-1 suppression in tumor cells on their survival in vitro and the effect of PAI-1 suppression in both tumor cells and host cells on tumorigenesis in vivo.

Methods

Cell Lines and Cell Culture

HT-1080 human fibrosarcoma, A549 human lung carcinoma, HCT-116 human colon carcinoma, and MDA-MB-231 human breast adenocarcinoma cell lines were obtained from American Type Culture Collection (ATCC; Manassas, VA). All cells were grown in monolayer cultures in RPMI-1640 medium (Mediatech Inc, Manassas, VA) supplemented with 10% fetal bovine serum (Hyclone, Logan, UT), 2 mM L-glutamine (Invitrogen, Carlsbad, CA), 100 μg/mL streptomycin (Mediatech Inc), and 100 units/mL penicillin (Mediatech Inc) in a humidified incubator (5% carbon dioxide, 95% air) at 37°C. The authenticity of all the cell lines was verified by short tandem repeat profile genotyping analysis (32).

Reagents

Purified mouse anti-human FasL neutralizing antibody (NOK-2 clone, 1:100 dilution) and a caspase-8 inhibitor (Z-IETD-FMK, 1:200 dilution) were purchased from BD Biosciences (San Diego, CA). Mouse anti-human Fas neutralizing antibody (ZB4 clone, 1:200 dilution) and uPA activity assay kit were from Millipore (Billerica, MA). Mouse IgG1 isotype control was from R&D Systems (Minneapolis, MN). Aprotinin (Bovine, Recombinant) was purchased from Calbiochem (San Diego, CA). Human recombinant plasminogen activator inhibitor-1 (stable mutant form with point mutations of K154T, Q319L, M354L, and N150H) was from Molecular Innovations Inc (Novi, MI). PAI-1 small molecule inhibitor PAI-039 (Tiplaxtinin) was from Axon MedChem (Groningen, The Netherlands). PAI-039 was dissolved in dimethyl sulfoxide at a stock concentration of 10 mM and stored at –20°C.

RNA Interference

Small Interference RNA (siRNA). Two duplex oligonucleotides encoding siRNA designed against human PAI-1 mRNA sequences (GenBank Accession number X12701) and a scrambled control siRNA were used in this study (QIAGEN Inc, Valencia, CA). The siRNA target sequences were as follows: PAI-1 siRNA 1: 5′-AAGGATGAGATCAGCACCACA-3′; PAI-1 siRNA 2: 5′-AAGCAGCTATGGGATTCAAGA-3′; scramble control (sc) siRNA: 5′-AATTCTCCGAACGTGTCACGT-3′. Tumor cells were transfected with 100 nM of PAI-1 siRNA or sc siRNA using Lipofectamine 2000 (Invitrogen) (for MDA-MB-231 cells) or Lipofectamine iMax transfection reagent (Invitrogen) (for all the other cells) according to the manufacturer's instructions.

Short Hairpin RNA (shRNA). For stable knockdown of PAI-1, oligonucleotide duplexes used in siRNA experiments were expressed as shRNA in a pLKO.1-TRC lentiviral vector (Addgene, Cambridge, MA) and packaged into lentiviral particles by the HEK293T producer cell line. Supernatants from HEK293T cells containing pLKO.1 PAI-1 shRNA or sc lentiviral particles were collected after 48–72 hours of incubation. Thirty percent confluent tumor cell cultures were transduced by being incubated overnight with viral supernatant in the presence of 8 μg/mL polybrene (Sigma Aldrich, St Louis, MO). The virus-containing medium was then removed, and fresh medium containing 1 μg/mL puromycin (Sigma Aldrich) was added. Pooled populations of puromycin-resistant tumor cells were obtained after 4–5 days selection without subcloning.

Cell Proliferation and Cytotoxicity Assay

Proliferation and cytotoxicity assays were performed in 96-well plates (1×10^5 – 2×10^5 cells per well), using the fluorescence-based CyQUANT direct cell proliferation assay kit (Invitrogen) according to the manufacturer's instructions. When indicated, PAI-039 was added to each well in 50 μL of medium.

Caspase Activation Assay

Caspase activity in cell lysates was determined using specific colorimetric assay kits of Caspase-3/CPP32 (Invitrogen), Caspase-8/FLICE (Invitrogen), and Caspase-9 (R&D Systems) according to the manufacturer's instructions. Briefly, tumor cells were collected and suspended in chilled cell lysis buffer (supplied with the kit); the mixtures were incubated on ice for 10 minutes and centrifuged at 12 000*g* for 10 minutes at 4°C. The protein concentration in the lysates was determined using a bicinchoninic acid protein assay kit (Pierce Biotechnology, Rockford, IL). The lysates (50 μg of protein) were transferred to a 96-well microplate and made to a final volume of 50 μL by the addition of lysate buffer. Fifty microliters of 2× reaction buffer containing 10 mM 1,4-dithiothreitol and 5 μL of caspase substrate (DEVD-*p*NA for caspase-3, IETD-*p*NA for caspase-8, and LEHD-*p*NA for caspase-9) were added to each well of the microplate. The microplate was incubated at 37°C for

24 hours, and the presence of the chromophore *p*NA released by the activated caspase in the lysates was determined by reading the absorbance at 405 nm in a microtiter plate reader (Synergy™ HT, Bio-Tek Instruments Inc, Winooski, VT). Samples without a substrate [substrate blank containing reaction buffer containing 1,4-dithiothreitol and caspase substrate] were used as background controls.

Fluorescence-Activated Cell Sorting Analysis

Annexin V Staining Assay. Apoptosis was evaluated by assessing the subdiploid DNA content and Annexin V binding, using the fluorescein isothiocyanate (FITC) Annexin V Apoptosis Detection Kit I (BD Biosciences) according to the manufacturer's instructions. Briefly, HT-1080, A549, HCT-116, and MDA-MB-231 tumor cells were collected and suspended in 100 μL of binding buffer at a final concentration of 0.5×10^6 cells per 50 μL. Five microliters of Annexin V–FITC and 5 μL of propidium iodide (PI, 20 μg/mL) were added to the cell suspension, and the mixture was incubated for 15 minutes at room temperature in the dark. The cells were then resuspended in 400 μL of binding buffer and analyzed by flow cytometry with band-pass filters of 525 ± 25 nm for FITC and 610 ± 20 nm for PI in a BD LSR II system (BD Biosciences) equipped with the DiVA software (Version 6.0; BD Biosciences).

Expression of Fas and FasL on Cell Surface. HT-1080, A549, HCT-116, and MDA-MB-231 cells were collected and resuspended in 1 mL of the buffer containing 5% fetal calf serum and 0.1% sodium azide in phosphate-buffered saline at a density of 1×10^6 cells/mL. Expression of Fas and FasL on the cell surface was detected by flow cytometry using mouse monoclonal anti-Fas (1:100 dilution, Enzo Life Sciences Inc, Farmingdale, NY) or anti-FasL (1:100 dilution, Enzo Life Sciences Inc) as a primary antibody and a FITC-conjugated horse anti-mouse IgG (Vector laboratories Inc, Burlingame, CA) as a secondary antibody. A mouse IgG primary antibody was used as a negative control.

Western Blot Analysis

HT-1080, A549, HCT-116, and MDA-MB-231 cells were lysed on ice for 15 minutes with a solution containing 50 mM Tris, 1% Triton X-100, 0.1% sodium dodecyl sulfate, 150 mM NaCl, and 1% of 100x Halt Protease and Phosphatase Inhibitor Cocktail (Thermo Scientifics, Rockford, IL). The cell lysates were then centrifuged at 12 000*g* for 15 minutes, and equal amounts of protein in the supernatants were resolved by electrophoresis on a 4%–20% Tris-Glycine precast gradient acrylamide gel (Invitrogen) and transferred to a 0.45-μm nitrocellulose membrane (Bio-Rad Laboratories, Hercules, CA). After blocking with 5% nonfat dry milk in Tris-buffered saline containing 0.05% Tween-20, the membranes were incubated overnight at 4°C with the following primary antibodies: a mouse monoclonal anti-human PAI-1 antibody (1:500 dilution; R&D Systems), a rabbit polyclonal anti-poly adenosine diphosphate-ribose polymerase (PARP) antibody (1:500 dilution; Cell Signaling Technology, Danvers, MA), and a mouse monoclonal anti-glyceraldehyde 3-phosphate dehydrogenase (GAPDH) antibody (1:1000 dilution; Santa Cruz Biotechnology, Santa Cruz, CA). Subsequently, membranes were incubated with a horseradish peroxidase–conjugated secondary antibody (1:3000 dilution; Vector Laboratories Inc), and the immunocomplexes were visualized on an autoradiography film (Denville Scientific Inc, Metuchen, NJ) using a chemiluminescent substrate kit (Pierce Biotechnology).

Measurement of PAI-1 Levels

Human and murine PAI-1 levels in the lysates of cultured cells and murine plasma were determined using commercially available enzyme-linked immunosorbent assay (ELISA) kits (American Diagnostica Inc, Stamford, CT) according to manufacturer's instructions.

Measurement of uPA Activities

Human uPA activities in total cell lysates of cultured cells were determined using the commercially available uPA activity assay kit (EMD Millipore Corporation, Billerica, MA) according to manufacturer's instructions.

Measurement of Plasmin Activities

Human plasmin activities in total cell lysates of cultured cells were determined according to the method described by Bekes et al. (33): to each well of the 96-well plate, cell lysate sample or positive control (human plasmin, no. 411, 7.5 units/mg; American Diagnostica Inc) was added, and sufficient sample buffer (50 mM Tris-HCl, pH 8.0) was added to bring the total volume to 80 μL; another 20 μL of chromogenic substrate of plasmin (5 mM, S-2251™; Chromogenix, Instrumentation Laboratory Company, Lexington, MA) was added to each well. The 96-well plate was then incubated at 37°C for 20 hours, and the presence of the chromophore *p*NA released by the active plasmin in the lysates was determined by reading the absorbance at 405 nm in a microtiter plate reader (Synergy™ HT, Bio-Tek Instruments Inc). Plasmin activities in the samples were calculated using a plasmin activity standard curve and expressed in milli units per mg of cell lysate.

Plasminogen/Fibrinogen Zymography for uPA

Plasminogen/fibrinogen zymography analysis of uPA activity was performed as previously described with minor modifications (34). Briefly, HT-1080 and HCT-116 cells were lysed on ice for 15 minutes with a solution containing 50 mM Tris, 1% Triton X-100, 0.1% sodium dodecyl sulfate, and 150 mM NaCl (without any protease or phosphatase inhibitors). The cell lysates were then centrifuged at 12 000*g* for 15 minutes, and equal amounts of protein in the supernatants were resolved by electrophoresis on the plasminogen plus fibrinogen gel without boiling; human urokinase (0.3 U, Calbiochem) was used as the positive control. The following components were incorporated into each plasminogen plus fibrinogen gel: 1.7 mL of double-distilled water, 1.5-mL Tris-HCl (pH 8.8), 2.2-mL 30% acrylamide/Bis Solution 29:1 (Bio-Rad Laboratories), 100-μL fibrinogen (10 mg/mL; Sigma Aldrich), 250-μL plasminogen (1.1 mg/mL; human plasma, Calbiochem), 50-μL ammonium persulfate, 10-μL tetramethylethylenediamine (TEMED; Bio-Rad Laboratories), and 60-μL 10% sodium dodecyl sulfate. The running buffer (pH 8.3) contained 0.5 M Tris, 0.38 M glycine, and 0.1% sodium dodecyl sulfate. After electrophoresis, the gels were rinsed with distilled water and washed twice for 30 minutes each using 2.5% Triton X-100 to remove sodium dodecyl sulfate. Gels were incubated for 16 hours at 37°C in the developing

buffer (0.1 M glycine, pH 8.0); the gels were stained with 0.25% coomassie brilliant blue, 50% methanol, and 40% acetic acid for 1 hour and then destained in the mixture of 50% methanol and 40% acetic acid.

Mouse Models and Xenograft Experiments

All mouse experiments were performed in accordance with protocols approved by the Institutional Animal Care and Usage Committee of Children's Hospital Los Angeles. Rag-1$^{-/-}$ PAI-1$^{+/+}$ wild-type (WT) and Rag-1$^{-/-}$ PAI-1$^{-/-}$ knockout (KO) immunodeficient mice were generated as previously described (28,35). Four- to 6-week-old female mice were used in this study, and mice were genotyped by polymerase chain reaction done on tail DNA using three primers specific for PAI-1 alleles (1): 5′-GAG TGG CCT GCT AGG AAA TTC ATT C-3′; (2) 5′-GAC CTT GCC AAG GTG ATG CTT GGC AAC-3′; (3) 5′-AAT GTG TCA GT120T TCA TAG CC-3′. One 400-bp band and one 190-bp band were detected in polymerase chain reaction products for PAI-1$^{+/+}$ mice and PAI-1$^{-/-}$ mice, respectively. MDA-MB-231 cells (2×10^6) were injected into the fourth mammary fat pad, and HT-1080 cells, A549 cells, or HCT-116 cells (5×10^6) were injected subcutaneously into the right flanks of mice (HT-1080: 9–15 mice per group; A549 and HCT-116: five mice in each group; MDA-MB-231: 5–8 mice in each group). After tumors became palpable, tumor size (length and width) was measured every 2–3 days using a vernier caliper, and the tumor volume was calculated using the modified ellipsoid formula: tumor volume (mm^3) = (width in mm)^2 × (length in mm) × $\pi/6$. When tumors reached the size of 1500 mm^3 or showed signs of ulceration, or when animals were found in distress, mice were killed by CO_2. Two hours before killing, mice were injected intraperitoneally with 4 mg/mouse bromodeoxyuridine (BrdU; Sigma Aldrich). After surgical resection, tumor tissue samples were cut in two halves; one half was fixed in 4% paraformaldehyde in phosphate-buffered saline overnight at 4°C before paraffin-embedding, and the other half was frozen in optimum cutting temperature formulation (VWR, Radnor, PA).

Murine Blood Collection

Blood samples were collected from anesthetized mice by the retro-orbital method (36) using a 75-mm heparinized hematocrit tube (Drummond Scientific Company, Broomall, PA). Whole blood was centrifuged in a 200Z gel-coated microcuvette tube (SARSTED Inc, Newton, NC), and the plasma was collected and stored at –20°C before being assayed for human PAI-1 and mouse PAI-1 detection by ELISA.

Immunohistochemistry

Terminal Nucleotidyl Transferase–Mediated Nick End Labeling (TUNEL) Staining and BrdU Staining. Paraformaldehyde-fixed, paraffin-embedded tumor tissue sections (5 μm) were immunostained for TUNEL using an in situ cell death detection kit (AP, Roche Diagnostics, Indianapolis, IN) followed by a substrate solution (Fuchsin + substrate-chromogen system, DAKO Corporation, Carpinteria, CA), and for BrdU using a BrdU Immunohistochemistry Kit (Millipore) according to the manufacturer's instructions. Images were acquired on a Zeiss wide-field Axioplan microscope (Oberkochen, Germany). The number of TUNEL-positive cells was counted manually in five fields per tumor section at 20× magnification. To determine the percentage of proliferative cells, the number of total nuclei and BrdU-positive nuclei was counted in five fields per tumor section at 20× magnification with MetaMorph 6.3 software (Molecular Devices Inc, Sunnyvale, CA).

Blood Vessel Staining. Optimal cutting temperature compound–embedded frozen tumor tissue sections (5 μm) were immunostained for blood vessels using a rat anti-mouse CD31 primary antibody (1:75 dilution, BD Biosciences) followed by a biotinylated goat anti-rat secondary antibody (1:200 dilution, Vector Laboratories Inc). Endogenous peroxidase activity was blocked by 0.3% H_2O_2, and Elite-ABC kit (Vector Laboratories Inc) was applied afterward. Visualization of antibody binding was carried out by diaminobenzidine (DAB, Sigma-Aldrich) staining, and sections were counterstained with Gill 3 hematoxylin (Sigma-Aldrich). The pixels of CD31-positive cells and the pixels of the whole tumor area were counted with MetaMorph 6.3 software in five fields per tumor at 20× magnification, and the microvessel densities were calculated as a percentage of positive pixels (37).

Statistical Analyses

Results were subjected to statistical analysis using GraphPad Prism version 5.00 for Windows (GraphPad Software Inc, San Diego, CA; www.graphpad.com). Nonlinear regression of inhibitory dose–response analysis was used to calculate the IC_{50} of PAI-039, the concentration causing 50% inhibition in cell viability. The Kaplan–Meier method was used to analyze event-free survival curves, and the differences in survival duration were determined using a log-rank test. An event was defined as tumor volume of at least 1500 mm^3 or tumor ulceration that necessitated killing of the animal. Analysis of variance was used to compare the differences among multiple groups. A two-sided unpaired Student *t* test was used to evaluate statistically significant differences between two groups. Results were expressed as mean ± 95% confidence intervals (error bars) with two independent experiments performed in triplicate in each experiment. A *P* value of less than .05 was considered statistically significant.

Results

Genetic Downregulation and Pharmacological Inhibition of PAI-1 and Spontaneous Apoptosis in Human Cancer Cell Lines

To test the hypothesis that tumor-derived PAI-1 has a similar antiapoptotic effect on tumor cells as the one reported by us (28) in ECs, we first suppressed PAI-1 expression by siRNA in human cancer cell lines and examined the effect on unstimulated (spontaneous) apoptosis using three different assays (PARP cleavage, caspase-3 activation, and Annexin V staining). We selected two human cancer cell lines with high levels of expression (HT-1080 fibrosarcoma and MDA-MB-231 breast cancer cells, which contain 491 and 368 ng of PAI-1/mg cellular protein, respectively) and two cell lines with low levels of expression (A549 lung adenocarcinoma and HCT-116 colon carcinoma cells, which contain 38 and 6 ng of PAI-1/mg cellular protein, respectively). As shown in Figure 1,

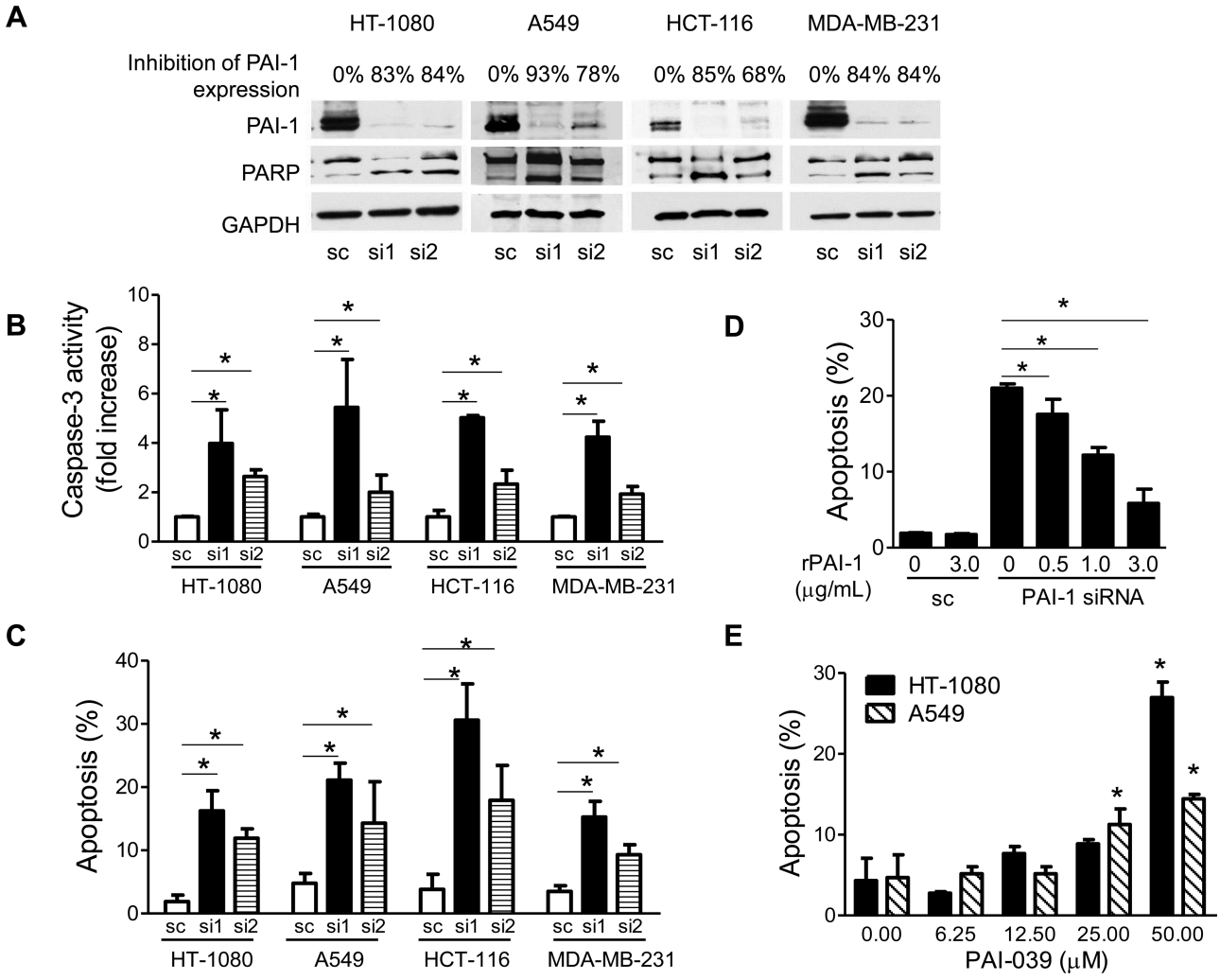

Figure 1. Inhibition of PAI-1 and induction of spontaneous apoptosis in human cancer cell lines. **A**) HT-1080, A549, HCT-116, and MDA-MB-231 cells transfected with PAI-1-specific siRNA #1, siRNA #2, or scramble control siRNA were examined after 72 hours for PAI-1 expression and PARP cleavage by western blot analysis. GAPDH served as the loading control. Data are representative of two independent experiments. The numbers indicated above the gel represent the percent decrease in PAI-1 expression upon scanning of the western blot data. **B**) Caspase-3 activity of cells treated as in (**A**). Data represent the mean fold increase relative to sc in caspase-3 activity for triplicate samples assayed in two separate experiments (mean fold increase vs sc: HT-1080, si 1, $P < .001$; si 2, $P < .001$; A549, si1, $P < .001$; si 2, $P = .004$; HCT-116, si1, $P < .001$; si 2, $P < .001$; MDA-MB-231: si1, $P < .001$; si 2, $P < .001$, two-sided Student *t* test). **C**) Cells treated as in (**A**) were examined for apoptosis by PI and Annexin V staining. Data represent the mean percentage of Annexin V–positive cells for triplicate samples assayed in two separate experiments (mean % vs sc: HT-1080, si 1, $P < .001$; si 2, $P < .001$; A549, si1, $P < .001$; si 2, $P = .004$; HCT-116, si1, $P < .001$; si 2, $P < .001$; MDA-MB-231: si1, $P < .001$; si 2, $P < .001$, two-sided Student *t* test). **D**) HT-1080 cells were transfected with PAI-1 siRNA or the scramble control siRNA in the presence or absence of rPAI-1, and apoptosis was determined after 72 h. The data represent the mean percentage of Annexin V–positive cells for triplicate samples assayed in two separate experiments. PAI-1 siRNA transfected samples plus rPAI-1 vs minus rPAI-1 (0.5 μg/mL rPAI-1, $P = .003$; 1.0 μg/mL rPAI-1, $P < .001$; 3.0 μg/mL rPAI-1, $P < .001$, two-sided Student *t* test). **E**) HT-1080 and A549 cells were treated with PAI-039 at indicated concentrations for 72 hours before being examined for apoptosis with PI and Annexin V staining. The data represent the mean percentage of Annexin V–positive cells for triplicate samples assayed. Similar results were observed in two independent experiments (PAI-039 treated samples vs DMSO-treated controls: HT-1080 cells, 50.00 μM PAI-039, $P < .001$; A549 cells, 25.00 μM PAI-039, $P = .001$, 50.00 μM PAI-039, $P < .001$, two-sided Student *t* test). PAI-1 = plasminogen activator inhibitor 1; rPAI-1 = recombinant PAI-1; siRNA = small interference RNA; sc = scramble control siRNA; si1 = siRNA 2; si2 = siRNA2; PI = propidium iodide; GAPDH = glyceraldehyde 3-phosphate dehydrogenase; PARP = poly adenosine diphosphate-ribose polymerase; DMSO = dimethyl sulfoxide. **Error bars** indicate 95% confidence intervals. **Asterisks** indicate statistically significant differences.

A, transfection of both siRNA sequences (si1 and si2) resulted in substantially lowered expression of cell-associated PAI-1 protein when compared with cells transfected with a sc sequence. Suppression of PAI-1 in these cells resulted in PAI-1 levels in the conditioned medium ranging from 0 (MDA-MB-231) to 145 ng/mL (HT-1080) (data not shown). The knockdown of PAI-1 expression was associated with an increase in PARP cleavage (Figure 1, A) and a statistically significant increase in caspase-3 activation (Figure 1, B) in all four cell lines (mean fold increase relative to control: HT-1080, si1: mean = 4.0, 95% CI = 2.6 to 5.3, $P < .001$; si2: mean = 2.6, 95% CI = 2.4 to 2.9, $P < .001$, Student *t* test). PAI-1 knockdown was also associated with a statistically significant increase in the percentage of Annexin V–positive cells (Figure 1, C) in all four cell lines (mean percentage of Annexin V–positive cells: HT-1080, si1: mean = 16.3%, 95% CI = 13.0% to 19.5%, $P < .001$; si2: mean = 11.9%, 95% CI = 10.4% to 13.4%, $P < .001$; sc:

mean = 1.9%, 95% CI = 0.9% to 2.9%). To prove the specificity of this proapoptotic effect by PAI-1 suppression through siRNA, we next tested whether the addition of human stable recombinant PAI-1 (rPAI-1) could reverse apoptosis. The concentrations of rPAI-1 were selected based on the basal levels of PAI-1 in the conditioned medium from the tumor cells transfected with sc (3.0 μg/mL in HT-1080 cells and 1.3 μg/mL in MDA-MB-231 cells). We demonstrated that the addition of human rPAI-1 to the culture medium of HT-1080 cells (Figure 1, D) and MDA-MB-231 cells (Supplementary Figure 1, available online) in which PAI-1 was knocked down by siRNA restored apoptosis to the similar low levels observed in the cells transfected with a scramble siRNA. Similarly, we observed that the addition of rPAI-1 (3.0 μg/mL) increased the level of cell-associated PAI-1 from 91 ng/mg protein to 476 ng/mg protein in PAI-1 knockdown (KD) HT-1080 cells. In HT-1080 cells, a dose-dependent effect of rPAI-1 on apoptosis reversal was observed at concentrations ranging from 0.5 to 3.0 μg/mL (Figure 1, D). This observation also pointed to an extracellular effect of PAI-1.

We subsequently applied a pharmacological approach besides this genetic approach to further test our hypothesis by examining the effect of PAI-039 (Tiplaxtinin), a small molecular PAI-1 inhibitor (38), on tumor cell apoptosis and cytotoxicity. These experiments demonstrated that inhibition of PAI-1 activity by PAI-039-induced apoptosis in a dose-dependent manner in HT-1080 and A549 cells (mean apoptosis levels, control [0 μM] vs 50 μM PAI-039: in HT-1080 cells, 4.3% vs 27.0%, difference = 22.7%, 95% CI = 20.5% to 24.9%, $P < .001$; in A549 cells, 4.7% vs 14.5%, difference = 9.8%, 95% CI = 7.9% to 11.6%, $P < .001$; Figure 1, E). PAI-039 also inhibited cell survival in HT-1080, A549, HCT-116, and MDA-MB-231 cells, with IC_{50} values of 28.4 μM, 35.7 μM, 32.4 μM, and 61.5 μM, respectively (Supplementary Figure 2, available online).

Taken together, the data indicate that PAI-1, through an extracellular effect, has a protective action on spontaneous apoptosis in cancer cells, as previously shown in EC.

Suppression of PAI-1 and Extrinsic Apoptosis in Tumor Cells

To test whether PAI-1 suppression in tumor cells involves the activation of the extrinsic apoptotic pathway, we examined the effect of PAI-1 knockdown on caspase-8 activation, a marker of extrinsic apoptosis, and the involvement of Fas and FasL, the key mediators in extrinsic apoptosis reported by us to be regulated by PAI-1 in EC (28). In support of an involvement of the extrinsic apoptotic pathway, we first demonstrated a statistically significant twofold to fivefold increase in caspase-8 activity in all four tumor cell lines tested (Figure 2, A) upon PAI-1 knockdown by siRNA when compared with respective scs (mean fold increase of caspase-8 activity relative to sc: PAI-1 siRNA, HT-1080 cells, mean = 2.3-fold, 95% CI = 1.8- to 2.9-fold, $P < .001$; A549 cells, 3.9-fold, 95% CI = 2.2- to 5.6-fold, $P < .001$; HCT-116 cells, mean = 6.8-fold, 95% CI = 4.9- to 8.7-fold, $P < .001$; MDA-MB-231 cells, 4.0-fold, 95% CI = 2.7- to 5.3-fold, $P < .001$).

Consistent with caspase-8 activation being critical, we showed that the addition of a caspase-8-specific inhibitor (Z-IETD-FMK) to tumor cells in which PAI-1 was suppressed by siRNA prevented the induction of apoptosis as shown by inhibition of PARP cleavage (Figure 2, B). We next asked the question whether the activation of extrinsic apoptosis observed upon PAI-1 downregulation involved Fas and FasL. We first demonstrated the expression of both Fas and FasL on the cell surface of all four cell lines (Figure 2, C) by flow cytometry. To verify the role of Fas and FasL, we then demonstrated an inhibition of PARP cleavage in PAI-1 knocked-down in HT-1080 and MDA-MB-231 cells in the presence of a blocking antibody against Fas (ZB-4) or FasL (NOK-2) or in the presence of both (Figure 2, D). However in HT-1080 cells, the levels of PARP cleavage upon PAI-1 suppression in the presence of Fas/FasL blocking antibodies remained higher (ratio of cleaved PARP/GAPDH = 1.9, 1.9, and 2.4, lanes 5–7, respectively, Figure 2, D) than the sc (ratio = 1.0), suggesting the possibility of a Fas/FasL-independent mechanism. Annexin V staining was also used to confirm the dependence of this effect on Fas/FasL-mediated extrinsic apoptosis. These data demonstrated a statistically significant, although not complete, decrease in the levels of apoptosis upon PAI-1 suppression in all four cell lines by either blocking Fas/FasL (mean apoptotic levels, PAI-1 siRNA vs PAI-1 siRNA + ZB4+NOK-2: HT-1080 cells, mean = 24.2% vs 10.4%, difference = –13.8%, 95% CI = –18.3% to –9.3%, $P = .001$; A549 cells, mean = 22.4% vs 9.8%, difference = –12.6%, 95% CI = –18.4% to –6.8%, $P = .001$; HCT-116 cells, mean = 28.5% vs 19.4%, difference = –9.1%, 95% CI = –12.3% to –5.9%, $P < .001$; MDA-MB-231 cells, mean = 16.9% vs 8.2%, difference = –8.7%, 95% CI = –11.4% to –6.1%, $P < .001$) or inhibiting caspase-8 activity (mean apoptotic levels, PAI-1 siRNA vs PAI-1 siRNA + Z-IEDT-FMK: HT-1080 cells, mean = 24.2% vs 13.7%, difference = –10.5%, 95% CI = –15.1% to –5.9%, $P < .001$; A549 cells, mean = 22.4% vs 12.9%, difference = –9.5%, 95% CI = –15.9% to –3.3%, $P = .007$; HCT-116 cells, mean = 28.5% vs 18.4%, difference = –10.1%, 95% CI = –12.9% to –7.2%, $P < .001$; MDA-MB-231 cells, mean = 16.9% vs 7.2%, difference = –9.7%, 95% CI = –13.4% to –6.1%, $P < .001$; Figure 2, E). The data indicate that PAI-1 protects tumor cells from Fas/FasL-mediated extrinsic apoptosis but do not rule out the possibility of an additional Fas/FasL-independent mechanism.

Role of Plasmin in Apoptosis

To test whether this antiapoptotic role of PAI-1 involves its antiproteolytic activity, we first examined the effects of PAI-1 knockdown on uPA and plasmin activities in HT-1080 cells (high PAI-1 levels) and HCT-116 cells (low PAI-1 levels). It is noteworthy that despite the difference in the amount of PAI-1 produced by these two cell lines, the activities of cell-associated uPA were similar (65.2 U/mg total protein and 58.6 U/mg total protein, respectively). Suppression of PAI-1 in both cell lines resulted in a statistically significant increase in cell-associated uPA (mean uPA activity per mg of total protein: sc vs PAI-1 siRNA: HT-1080 cells, mean = 65.2 U vs 131.1 U, difference = 65.8 U, 95% CI = 49.3 U to 82.4 U, $P < .001$; HCT-116 cells, mean = 58.6 U vs 100.6 U, difference = 42.0 U, 95% CI = 31.3 U to 52.7 U, $P < .001$; Figure 3, A, upper panel). The increase in uPA activity upon PAI-1 suppression was confirmed by plasminogen/fibrinogen zymography, which demonstrated an increase in high molecular weight uPA (~50 KD) upon PAI-1 suppression in HT-1080 and

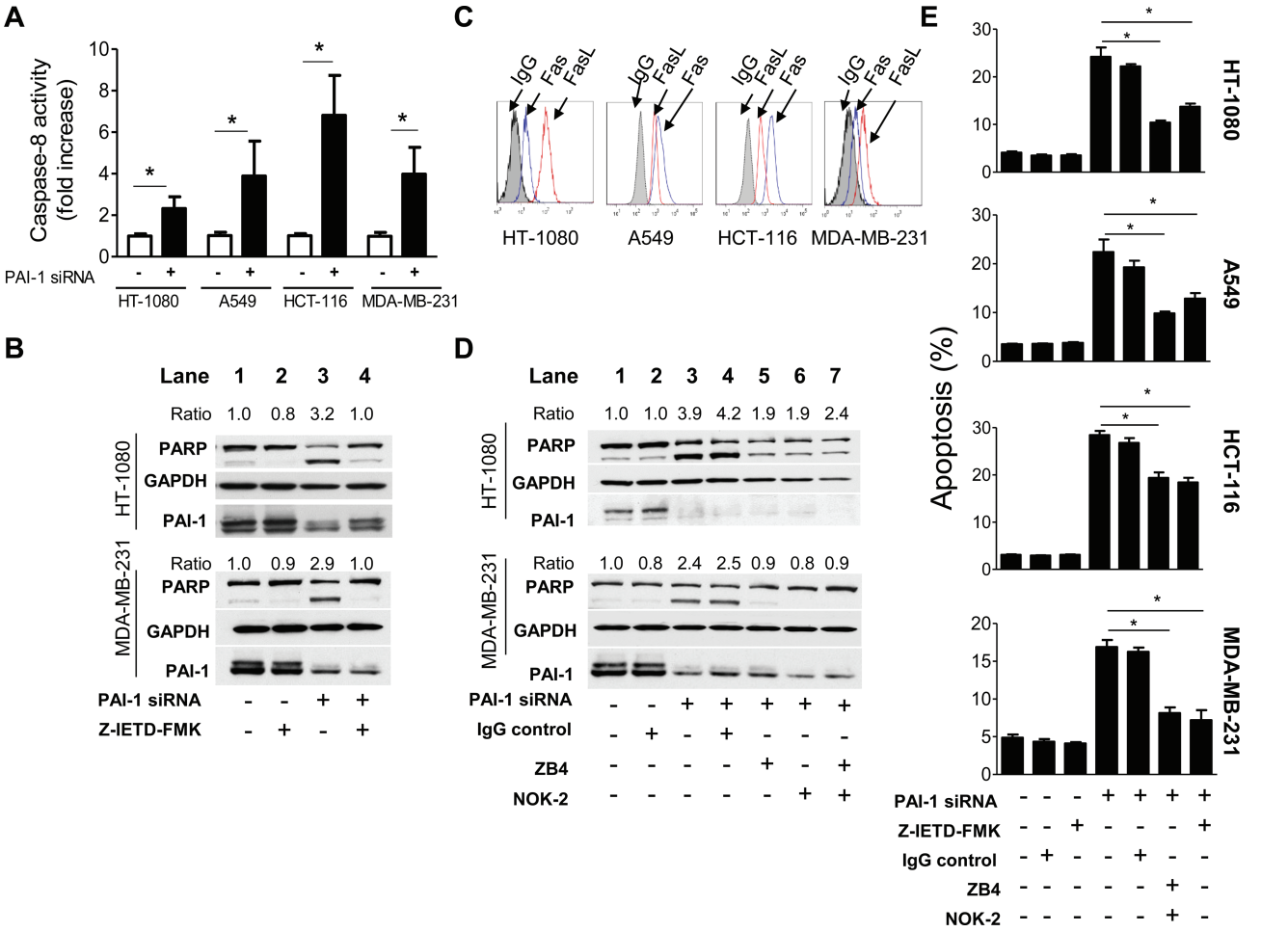

Figure 2. Suppression of PAI-1 and extrinsic apoptosis in tumor cells. **A**) HT-1080, A549, HCT-116, and MDA-MB-231 cells transfected with PAI-1 siRNA (**solid bars**) or the scramble control siRNA (**open bars**) were examined after 72 hours for caspase-8 activity using a colorimetric assay. Data represent the mean fold increase in caspase-8 activity for triplicate samples assayed in two separate experiments (mean fold increase vs sc: HT-1080 cells, $P < .001$; A549 cells, $P < .001$; HCT-116 cells, $P < .001$; MDA-MB-231 cells, $P = .005$, two-sided Student *t* test). **B**) HT-1080 and MDA-MB-231 cells were pretreated with or without a caspase-8 inhibitor (Z-IETD-FMK, 40 μM) for 1 hour before being transfected, and Z-IETD-FMK was readded to the medium after transfection. Cells were examined after 72 hours for PAI-1 expression and PARP cleavage by western blot analysis. Data are representative of two independent experiments. The cleaved PARP expression was normalized to GAPDH (as loading control) levels and expressed as relative ratio. The samples transfected with scramble control siRNA without the treatment of Z-IETD-FMK were set to 1.0. **C**) HT-1080, A549, HCT-116, and MDA-MB-231 cells were examined for Fas and FasL expression by flow cytometry. Representative data of the expression of Fas and FasL at the cell surface are shown. A mouse IgG (**gray area**) was used as a negative control. **D**) HT-1080 and MDA-MB-231 cells were pretreated with or without an anti-Fas neutralizing antibody ZB4 (5 μg/mL), an anti-FasL neutralizing antibody NOK-2 (5 μg/mL), or the combination for 1 hour before being transfected, and antibodies (ZB4 or NOK-2 or both) were readded to the medium after transfection. Cells were examined after 72 hours for PAI-1 expression and PARP cleavage by western blot analysis. Data are representative of two independent experiments. The cleaved PARP expression was normalized to GAPDH levels and expressed as relative ratio. The values of the samples transfected with scramble control siRNA without the treatment of ZB4 or NOK-2 were set to 1.0. **E**) HT-1080, A549, HCT-116, and MDA-MB-231 cells treated as in (**B**) were tested for apoptosis after 72 hours by staining tumor cells with propidium iodide (PI) and Annexin V using flow cytometry. Data represent the mean percentage of Annexin V–positive cells for triplicate samples assayed in at least two separate experiments (PAI-1 siRNA–transfected samples plus ZB4+NOK-2 or Z-IETD-FMK vs PAI-1 siRNA–transfected samples alone: HT-1080, ZB4+NOK-2, $P = .001$; Z-IETD-FMK, $P < .001$; A549, ZB4+NOK-2, $P = .001$; Z-IETD-FMK, $P = .007$; HCT-116, ZB4+NOK-2, $P < .001$; Z-IETD-FMK, $P < .001$; MDA-MB-231, ZB4+NOK-2, $P < .001$; Z-IETD-FMK, $P < .001$, two-sided Student *t* test). PAI-1 = plasminogen activator inhibitor 1; siRNA = small interference RNA; sc = scramble control siRNA; PI = propidium iodide; GAPDH = glyceraldehyde 3-phosphate dehydrogenase; PARP = poly adenosine diphosphate-ribose polymerase; FasL = Fas ligand. **Error bars** indicate 95% confidence intervals. **Asterisks** indicate statistically significant differences.

HCT-116 cells (Figure 3, A, lower panel). This increase in uPA activity was associated with a corresponding increase in cell-associated plasmin activity as shown in Figure 3, B (mean plasmin activity per mg of total protein: sc vs PAI-1 siRNA: HT-1080 cells, mean = 1.5 mU vs 4.1 mU, difference = 2.6 mU, 95% CI = 2.2 to 2.9 mU, $P < .001$; HCT-116 cells, mean = 2.0 mU vs 4.3 mU, difference = 2.3 mU, 95% CI = 1.9 to 2.7 mU, $P < .001$).

To demonstrate a link between plasmin activity and tumor cell apoptosis, we tested the effect of plasmin inhibition by aprotinin on apoptosis in HT-1080 cells, in which PAI-1 was suppressed by siRNA. The data indicated that when added at a concentration of 100 μg/mL, aprotinin almost completely abolished the levels of cell-associated plasmin activity (mean plasmin activity per mg of total protein: PAI-1 siRNA vs PAI-1 siRNA + 100 μg/mL aprotinin:

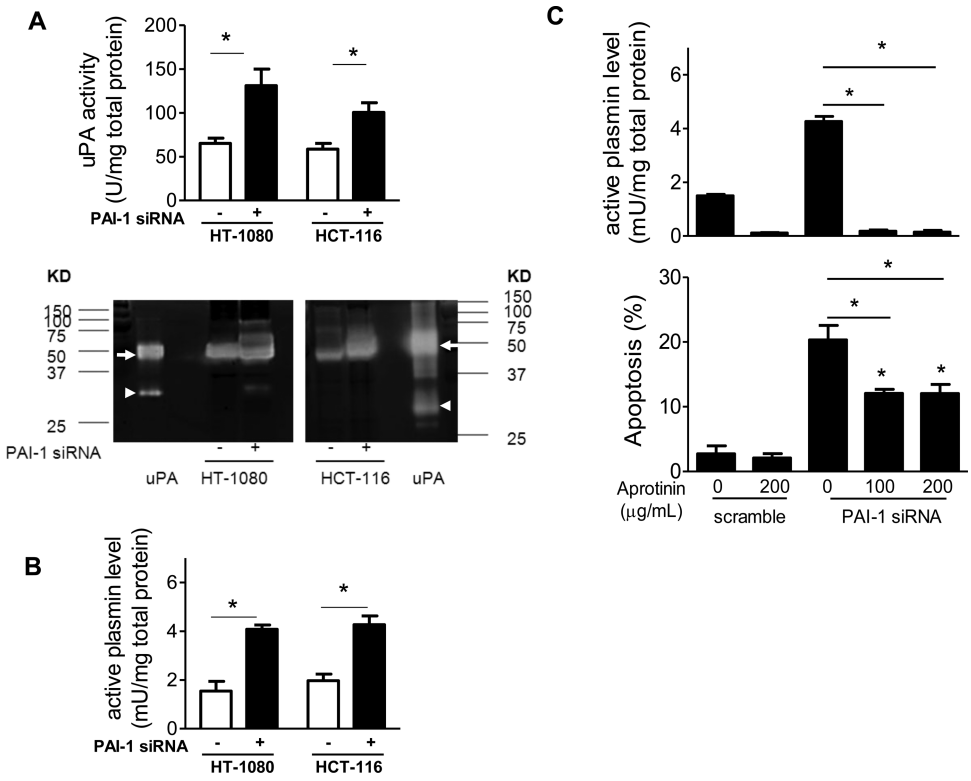

Figure 3. Role of plasmin in apoptosis. **A**) HT-1080 cells transfected with PAI-1 siRNA (**solid bars**) or the scramble control siRNA (**open bars**) were examined after 72 hours for uPA activity in cell lysates using the uPA activity assay kit (upper panel) or plasminogen/fibrinogen zymography (lower panel). In the upper panel, the **bar graphs** represent the mean units (U) of uPA per mg of total protein for triplicate samples assayed in two separate experiments (PAI-1 siRNA vs sc: HT-1080, $P = .004$; HCT-116, $P < .001$, two-sided Student t test). In the lower panel, the **clear bands** represent active uPA in the cell lysates, and human uPA from urine containing high molecular weight (50 KD, **arrow**) and low molecular weight uPA (35KD, **arrow head**) was added as the positive control. **B**) Cells treated as described in (**A**) were examined for plasmin activity in the cell lysates using the assay as described in "Methods." The **bar graphs** represent the mean milli units (mU) of plasmin per mg of total protein for triplicate samples assayed in two separate experiments (PAI-1 siRNA vs sc: HT-1080, $P < .004$; HCT-116, $P < .001$, two-sided Student t test). **C**) HT-1080 cells were transfected with PAI-1 siRNA or scramble control siRNA in the presence or absence of aprotinin; after 72 hours, cell-associated plasmin activity in the cell lysates was determined (upper panel), and apoptosis was assessed by PI and Annexin V staining (lower panel) using flow cytometry. In the upper panel, **bar graphs** represent the mean plasmin activity in mU per mg of total protein for triplicate samples assayed in two separate experiments (PAI-1 siRNA–transfected samples in the presence of 100 or 200 μg/mL aprotinin vs PAI-1 siRNA–transfected samples alone: 100 μg/mL aprotinin, $P < .001$; 200 μg/mL aprotinin, $P < .001$, two-sided Student t test). In the lower panel, **bar graphs** represent the mean percentage of Annexin V–positive cells from triplicate samples assayed in two separate experiments (PAI-1 siRNA–transfected samples in the presence of 100 or 200 μg/mL aprotinin vs PAI-1 siRNA–transfected samples alone: 100 μg/mL aprotinin, $P < .001$; 200 μg/mL aprotinin, $P < .001$; PAI-1 siRNA–transfected samples in the presence of 100 or 200 μg/mL aprotinin vs sc: 100 μg/mL aprotinin, $P < .001$; 200 μg/mL aprotinin, $P < .001$, two-sided Student t test). PAI-1 = plasminogen activator inhibitor 1; siRNA = small interference RNA; sc = scramble control siRNA; uPA = urokinase plasminogen activator; KD = kilo Dalton; PI = propidium iodide. **Error bars** indicate 95% confidence intervals. **Asterisks** indicate statistically significant differences.

mean = 4.3 mU vs 0.2 mU, difference = –4.1 mU, 95% CI = –4.2 to –4.0 mU, $P < .001$; Figure 3, C, upper panel). The addition of aprotinin also statistically significantly decreased the percentage of apoptotic cells in PAI-1 KD cells (mean apoptotic levels, PAI-1 siRNA vs PAI-1 siRNA + 100 μg/mL aprotinin: mean = 20.3% vs 12.0%, difference = –8.3%, 95% CI = –10.0% to –6.6%, $P = .001$; Figure 3, C, lower panel) but failed to return the level of apoptosis to basal levels in control cells even when used at a concentration of 200 μg/mL. These data indicate that plasmin is involved in inducing apoptosis in tumor cells upon PAI-1 downregulation, but they also point to the presence of a plasmin-independent mechanism.

Decreased Viability of Stable PAI-1 shRNA Expressing Tumor Cells

To stably knock down endogenous PAI-1 expression, HT-1080, A549, HCT-116, and MDA-MB-231 tumor cells were transduced with lentiviral particles containing the pLKO.1-TRC lentiviral vector coding for PAI-1 shRNAs (sc, sh1 and sh2). In these stable PAI-1 knockdown cells, the inhibition of PAI-1 expression ranged from 10% to 84% as a function of the cell line and the shRNA construct as shown by western blot analysis (Supplementary Figure 3, A, available online). We observed a statistically significant decrease in cell DNA content by fluorescence-based CyQUANT direct cell proliferation assay kit in PAI-1 shRNA#1-engineered HT-1080, A549, HCT-116, and MDA-MB-231cells on both day 3 and day 5 or 6 when compared with their scramble shRNA-engineered counterparts (Supplementary Figure 3, B, available online).

Inhibition of Tumorigenesis of Xenotransplanted HT-1080 Cells by Suppression of Host- and Tumor-derived PAI-1

Our data (Figure 1, D and Supplementary Figure 1, available online) indicate that the addition of exogenous rPAI-1 reverses apoptosis in cells in which endogenous PAI-1 was suppressed.

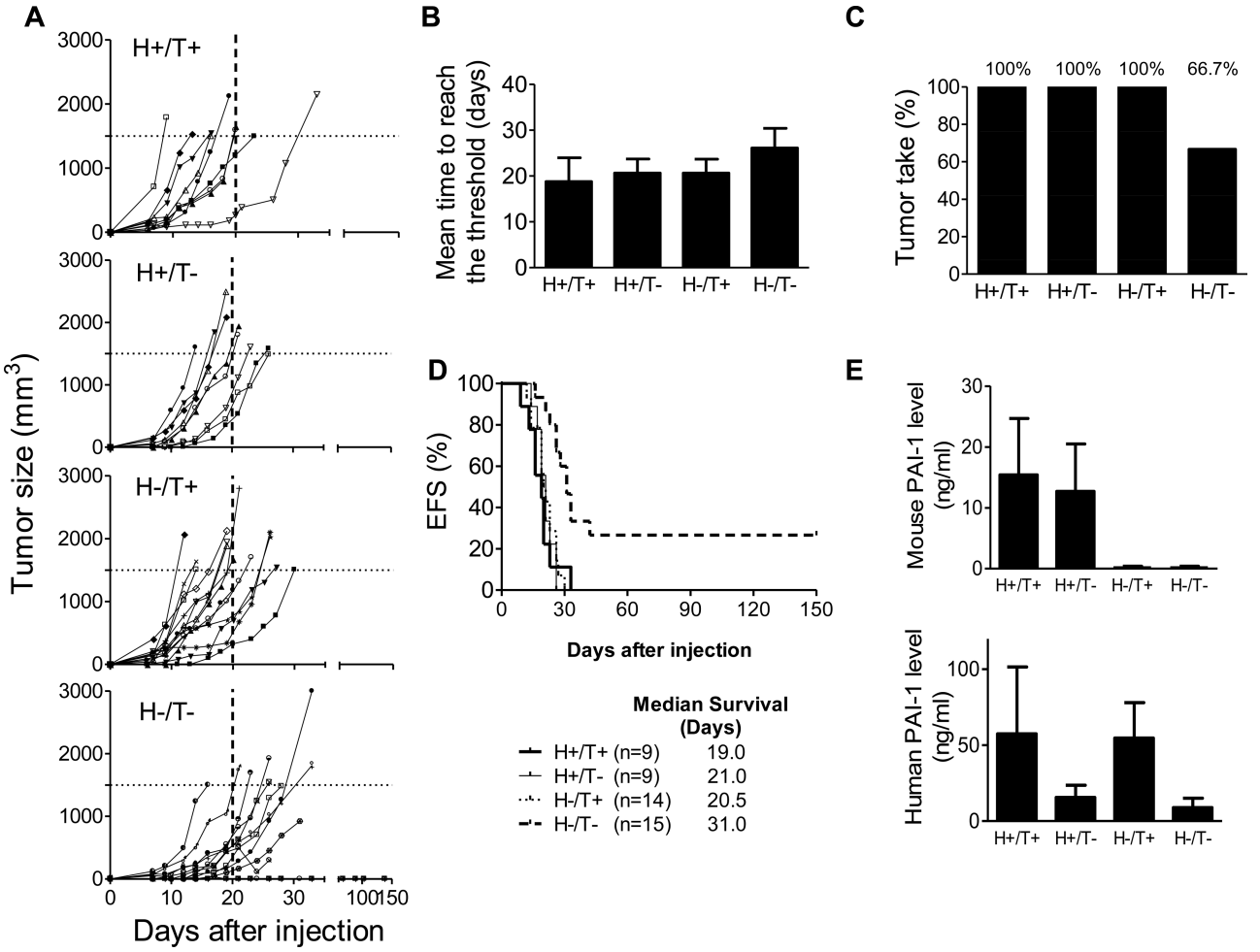

Figure 4. Inhibition of tumorigenesis of xenotransplanted HT-1080 cells by suppression of tumor- and host-derived plasminogen activator inhibitor-1 (PAI-1). **A**) HT-1080 cells stably transduced with PAI-1shRNA (T–) or scramble control shRNA (T+) producing lentiviral vector were injected subcutaneously into the right flank of 6- to 8-week-old female Rag-1$^{-/-}$ PAI-1$^{+/+}$ mice (H–) or Rag-1$^{-/-}$ PAI-1$^{-/-}$ mice (H+). Group H+/T+, n = 9; group H+/T–, n = 9; group H–/T+, n = 14; group H–/T–, n = 15. Mice were killed once the tumor volume was greater than or equal to 1500 mm^3 (**horizontal dotted line**). Data represent the volume of each individual tumor over time. **B**) Mean time for tumors in each group to reach a tumor volume of greater than or equal to 1500 mm^3 (P = .047; one-way ANOVA test). **C**) The percentage of mice developing tumors (tumor take) in each experimental group. **D**) EFS curve (Kaplan–Meier survival among groups: P = .002, log rank test) and median survival time of mice in each group over time. An event was defined as tumor volume greater than or equal to 1500 mm^3 or tumor ulceration that necessitated the death of the animal. **E**) Mean plasma levels of murine PAI-1 (upper panel) and human PAI-1 (lower panel) in each group of mice at the time of killing. Data are shown as mean of murine or human PAI-1 concentration (ng/mL) (group H+/T+, n = 6; group H+/T–, n = 6; group H–/T+, n = 10; group H–/T–, n = 7). PAI-1 = plasminogen activator inhibitor-1; shRNA = short hairpin RNA; ANOVA = analysis of variance between groups; EFS = event-free survival. **Error bars** indicate 95% confidence intervals.

These data thus pointed to an extracellular function of PAI-1 in protecting tumor cells from extrinsic apoptosis. We therefore postulated that host-derived PAI-1 may compensate for the lack of tumor-derived PAI-1 and that only in an absence or sufficient decrease in both host- and tumor-derived PAI-1, there would be a sizable inhibition of tumorigenesis in vivo. We initially tested this hypothesis in HT-1080 cells (transduced with either PAI-1shRNA #1 or the scramble shRNA lentiviral vector) that were subcutaneously xenotransplanted in immunodeficient Rag-1$^{-/-}$ PAI-1$^{-/-}$ mice or in their WT counterparts (Rag-1$^{-/-}$ PAI-1$^{+/+}$ mice). Four different experimental groups were generated as follows: scramble tumor cells in WT mice (host [H]+/tumor [T]+) (n = 9 per group), PAI-1 shRNA knockdown tumor cells in PAI-1 WT mice (H+/T–) (n = 9 per group), scramble tumor cells in PAI-1 KO mice (H–/T+) (n = 14 per group), and PAI-1 shRNA KD tumor cells in PAI-1 KO mice (H–/T–) (n = 15 per group). Mice were monitored for primary tumor formation, tumor volume, and survival for 150 days. The tumor take (the percentage of mice developing tumors) and mean time for a tumor to reach the threshold volume of 1500 mm^3 were calculated. Both human and mouse PAI-1 levels in the mouse plasma were also measured.

We observed a statistically significant difference in tumor growth between tumors of group H+/T+, H+/T– and H–/T+ mice, which reached a volume threshold of 1500 mm^3 in an average of 18.8 days (95% CI = 13.7 to 24.0 days), 20.7 days (95% CI = 17.6 to 23.7 days), and 20.6 days (95% CI = 17.6 to 23.7 days), respectively, and tumors of group H–/T– mice, which reached the threshold volume in an average of 25.8 days (95% CI = 20.9 to 30.6 days) (Figure 4, B).

Furthermore, no tumors were detected in five out of 15 mice in group H–/T–, resulting in a tumor take of 66.7%, compared with a 100% in all the other groups (Figure 4, C). Consistent with the need to inhibit PAI-1 in both tumor cells and in host cells to affect tumorigenesis, we observed a statistically significant increase in survival only in group H–/T– mice ($P = .002$, log-rank test) with a prolonged median survival time of 31 days when compared to 19–21 days in the other three groups (Figure 4, D).

The levels of host-derived (murine) PAI-1 and tumor-derived PAI-1 in murine plasma at the time of death in these four groups of mice were also determined (Figure 4, E). In the H+/T+ group, the mean murine PAI-1 level was 15.4 ng/mL (95% CI = 6.1 to 24.7 ng/mL), and the mean human PAI-1 was 57.6 ng/mL (95% CI = 13.6 to 101.5 ng/mL). In H+/T– group, the mean murine and human PAI-1 levels were 12.7 ng/mL (95% CI = 4.9 to 20.5 ng/mL) and 15.6 ng/mL (95% CI = 7.5 to 23.7 ng/mL), respectively. In H–/T+ group, the mean murine and human PAI-1 levels were 0.14 ng/mL (95% CI = –0.11 to 0.39 ng/mL; within the error range of detection of this assay) and 54.7 ng/mL (95% CI = 31.3 to 78.1 ng/mL), respectively. In H–/T– group, the mean murine and human PAI-1 levels were 0.11 ng/mL (95% CI = –0.08 to 0.32 ng/mL; within the error range of detection of this assay) and 8.9 ng/mL (95% CI = 2.6 to 15.1 ng/mL), respectively. The detection of human (tumor-derived) PAI-1 in the plasma from the 10 mice in the H–/T– group that developed tumors indicates that PAI-1 suppression was incomplete. Notably, human PAI-1 was not detected in the five mice that did not develop tumors. The fact that we never observed tumor formation in the absence of detectable human PAI-1 in the plasma in this group of mice suggests that PAI-1 expression was necessary for tumor growth. Together the data suggest that host- and tumor-derived PAI-1 may compensate for each other, and inhibition of both sources of PAI-1 was required to inhibit tumorigenesis.

HT-1080 tumors from these four groups of mice were then examined for apoptosis (TUNEL staining), proliferation (BrdU incorporation), and angiogenesis (CD31 expression) (Figure 5). This analysis revealed a statistically significant increase in cell apoptosis and a statistically significant decrease in cell proliferation in tumors derived from the H–/T– group of mice, when compared with tumors from the H+/T+ group (mean number of TUNEL-positive cells per field = 18.8 in H+/T+ group vs 57.1 in H–/T– group, difference = 38.3, 95% CI = 26.7 to 49.9, $P = .001$; mean percentage of BrdU positive nuclei = 31.8% in H+/T+ group vs 12.9% in H–/T– group, difference = –18.9%, 95% CI = –18.0% to –19.7%, $P = .004$). Tumors from the H+/T– group of mice also showed a decrease in BrdU-positive cells, but these differences were not statistically significant when compared with tumors of H+/T+ group, which is consistent with the inhibitory effect of PAI-1 KD on DNA content observed in vitro (Supplementary Figure 3, B, available online) being dependent on PAI-1 (produced by the host cells in this case) and not intrinsically related to the transduced cell line. There was also a statistically significant decrease in angiogenesis (microvessel density) in tumors from the H–/T– group of mice when compared with tumors from the H+/T+ group (mean percentage of microvessel density = 13.5% in H+/T+ group vs 7.4% in H–/T– group, difference = –6.1%, 95% CI = –9.8% to –2.4%, $P = .006$). Altogether the data indicate that a suppression of PAI-1 in both tumor cells and host cells is required to inhibit tumorigenesis and that the effect of PAI-1 inhibition on tumorigenesis involves a combination of antiproliferative, proapoptotic, and antiangiogenic activities.

Inhibition of A549, HCT-116, and MDA-MB-231 Tumorigenesis in the Absence of Host- and Tumor-Derived PAI-1

To confirm the inhibitory effect of PAI-1 suppression on tumorigenesis in other tumor cell lines, we xenotransplanted A549, HCT-116, and MDA-MB-231 cells transduced with the scramble shRNA lentiviral vector in Rag-$1^{-/-}$ PAI-$1^{+/+}$ mice (H+/T+, n = 5 per group) and cells transduced with PAI-1 shRNA#1 in Rag-$1^{-/-}$ PAI-$1^{-/-}$ mice (H–/T–, n = 5, 5, and 8 per group, respectively) and tested these two experimental groups of mice for primary tumor formation (Figure 6, A) and event-free survival (Figure 6, B).

As shown with HT-1080 cells, we observed a statistically significant inhibition of tumor growth in PAI-1 knockout mice xenotransplanted with PAI-1 knockdown A549 and HCT-116 tumor cells (H–/T– groups of mice) when compared with PAI-1 WT mice transplanted with A549 and HCT-116 tumor cells transduced with the control shRNA (H+/T+ group). The mean time to reach the volume threshold of 1500 mm^3 was 44.6 days in group H+/T+ vs 55.2 days in group H–/T– of A549 tumor cells (difference = 10.6 days, 95% CI = 7.9 to 13.3 days, $P = .05$) and 21.4 days in group H+/T+ vs 36.0 days in group H–/T– of HCT-116 tumor cells (difference = 14.6 days, 95% CI = 13.9 to 15.0 days, $P = .002$). Accordingly, mice in group H–/T– had a prolonged survival when compared with mice from group H+/T+ mice (median survival, group H+/T+ vs group H–/T–, A549: 45 days vs 55 days, $P = .048$, HCT-116: 21 days vs 35 days, $P = .004$; log-rank test). In all H–/T– group mice that developed tumors, human PAI-1 was detected in the plasma, indicating a failure of the shRNA to completely suppress PAI-1 expression, as seen in HT-1080 tumors. In MDA-MB-231 tumor-bearing mice, we observed—as with HT-1080 tumors—an absence of tumor take in two out of eight mice in group H–/T– even 180 days after tumor cell injection. As was the case in HT-1080 tumors, human PAI-1 in the plasma of these two mice was not detected (Supplementary Figure 4, available online).

In conclusion, these data demonstrate that in the absence of host-derived PAI-1 and upon a decrease of tumor-derived PAI-1, there is a statistically significant inhibition of tumorigenesis that is associated with a decrease in angiogenesis, an inhibition of cell proliferation, and an increase in host and tumor cell apoptosis. The data also demonstrate that host-derived PAI-1 can compensate for a decrease in tumor-derived PAI-1 and vice-versa and that the protumorigenic role of PAI-1 combines a prosurvival effect on both tumor cells and EC.

Discussion

Genetic and pharmacological inhibition of PAI-1 in four human tumor cell lines increased spontaneous apoptosis, which was blocked in the presence of recombinant PAI-1 and a caspase-8 inhibitor, and was partially attenuated by Fas/FasL neutralizing antibodies and a plasmin inhibitor-aprotinin. PAI-1 KO mice implanted with PAI-1 KD HT-1080 cells had decreased

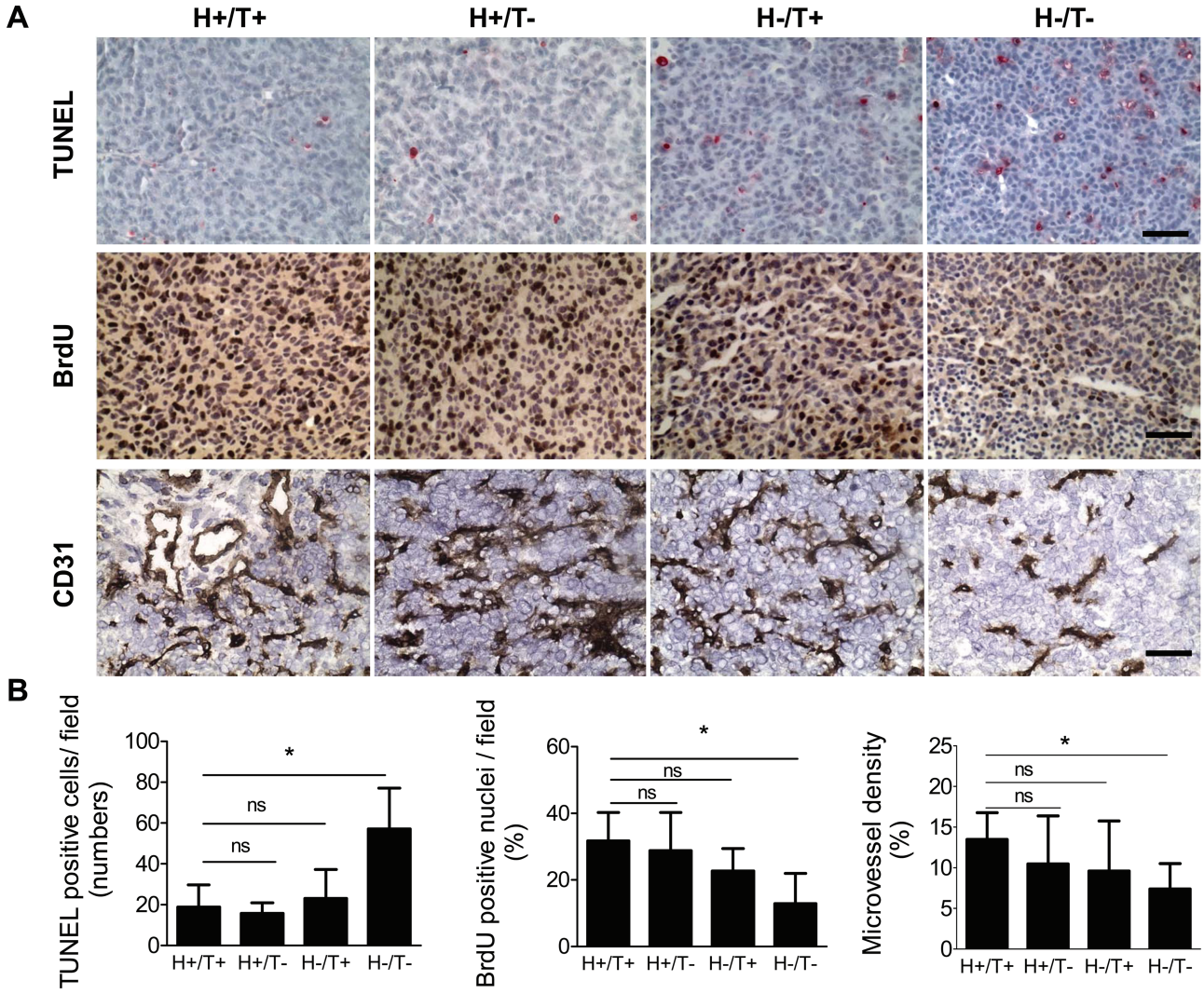

Figure 5. Increase in apoptosis, decrease in proliferation, and inhibition of angiogenesis in the absence of host- and tumor-derived PAI-1 in HT-1080 tumors. **A**) HT-1080 cells stably expressing PAI-1shRNA (T–) or scramble control shRNA (T+) were injected subcutaneously into the right flank of 6- to 8-week-old female Rag-1$^{-/-}$ PAI-1$^{+/+}$ mice (H–) or Rag-1$^{-/-}$ PAI-1$^{-/-}$ mice (H+). Representative immunohistochemical staining of HT-1080 tumor samples in the four experimental groups (H+/T+, H+/T–, H–/T+, H–/T–) for **top**) TUNEL, **middle**) BrdU, and **bottom**) CD31. The data show cell nuclei in **blue**, apoptotic nuclei in **red**, and proliferative cell nuclei and blood vessels in **brown** (×40 magnification, scale bar = 50 μm). **B**) **Left**) TUNEL-positive cells were counted in five randomly chosen fields at ×20 magnification in one section for each tumor. The data represent the mean TUNEL-positive cells per field (number of tumors examined in each group: group H+/T+, n = 9; group H+/T–, n = 9; group H–/T+, n = 8; group H–/T–, n = 8). One-way ANOVA test was first applied (P < .001), and two-sided Student t test was then applied for comparisons between two groups (H+/T+ vs H–/T–, P = .45, ns; H+/T– vs H–/T–, P = .49, ns; H–/T+ vs H–/T–, P = .001). **Middle**) BrdU-positive nuclei and total nuclei were counted in five randomly chosen fields at ×20 magnification in one section for each tumor. The data represent the mean percentage of BrdU-positive nuclei of the total nuclei counted (number of tumors examined in each group: group H+/T+, n = 6; group H+/T–, n = 7; group H–/T+, n = 6; group H–/T–, n = 5). One-way ANOVA test was first applied (P = .011), and two-sided Student t test was then applied for comparisons between two groups (H+/T+ vs H–/T–, P = .61, ns; H+/T– vs H–/T–, P = .07, ns; H–/T+ vs H–/T–, P = .004). **Right**) The number of CD31-positive pixels and total number of pixels in the same area were counted using MetaMorph 6.3 software in five randomly chosen fields at ×20 magnification in one section for each tumor. The mean microvessel density was calculated as the mean percentage of CD31-positive pixels per field (number of tumors examined in each group: group H+/T+, n = 4; group H+/T–, n = 3; group H–/T+, n = 3; group H–/T–, n = 5). One-way ANOVA test was first applied (P = .02), and two-sided Student t test was then applied for comparisons between two groups (H+/T+ vs H–/T–, P = .13, ns; H+/T– vs H–/T–, P = .07, ns; H–/T+ vs H–/T–, P = .006). PAI-1 = plasminogen activator inhibitor-1; shRNA = short hairpin RNA; TUNEL = terminal nucleotidyl transferase–mediated nick end labeling; BrdU = bromodeoxyuridine; ANOVA = analysis of variance between groups; ns = not statistically significant. **Error bars** indicate 95% confidence intervals. **Asterisks** indicate statistically significant differences.

tumorigenesis and prolonged survival compared with control mice, and their tumors exhibited decreased cell proliferation and angiogenesis and increased apoptosis. Furthermore, five of 15 PAI-1 KO mice implanted with PAI-1 KD HT-1080 cells never developed tumors. A similar inhibition of tumorigenesis was observed in PAI-1 KO mice implanted with PAI-1 KD A549, HCT-116, and MDA-MB-231 cells.

The mechanisms to explain the paradoxical activity of PAI-1 in cancer progression have primarily pointed to an effect on host-derived cells and in particular on EC where PAI-1 has been shown to have a proangiogenic activity by promoting EC migration and inhibiting Fas/FasL-mediated apoptosis (25,27,28,39,40). The role of PAI-1 in tumor cells initially focused on an antitumor activity by its inhibitory function on tumor invasion and metastasis (41).

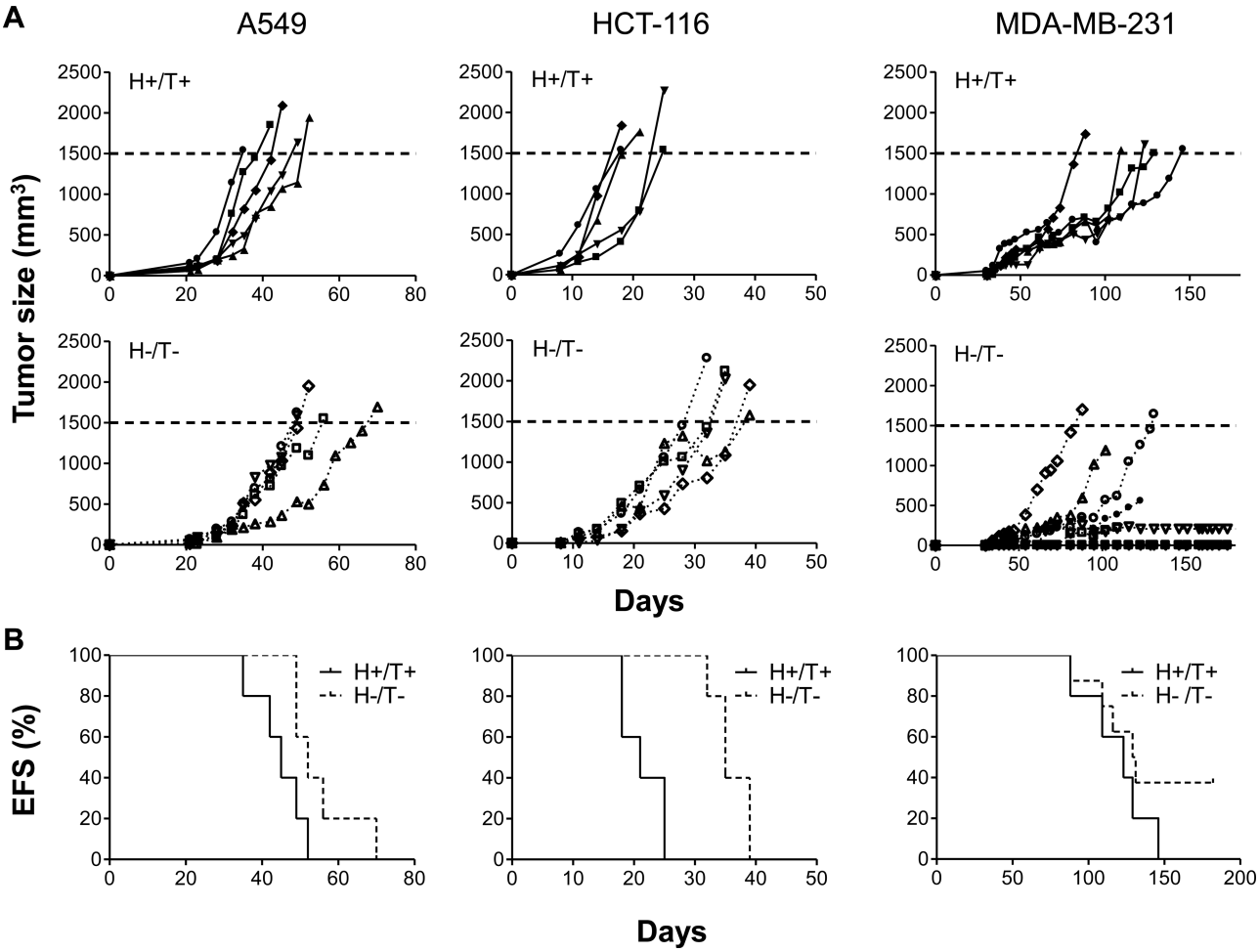

Figure 6. Inhibition of A549, HCT-116, and MDA-MB-231 tumorigenesis in the absence of host- and tumor-derived PAI-1. A549, HCT-116, and MDA-MB-231 cells stably expressing PAI-1 shRNA (T–) or scramble control shRNA (T+) were injected into 6- to 8-week-old female PAI-1$^{+/+}$ Rag-1$^{-/-}$ mice (H–) and PAI-1$^{-/-}$ Rag-1$^{-/-}$ mice (H+), respectively, to generate two different experimental groups: PAI-1 scramble cells in PAI-1 wild-type host (H+/T+), and PAI-1 knockdown cells in PAI-1 knockout host (H–/T–). N = 5 in each group of mice except in MDA-MB-231 H–/T– group where n = 8. **A**) The data represent the volume of individual tumors over time in each group for the three tumor cell lines tested. Mice were killed once the tumor volume was greater than or equal to 1500 mm^3 (**horizontal dotted line**). Data represent the volume of each individual tumor over time. **B**) The data represent the EFS curve (Kaplan–Meier survival between group H+/T+ and group H–/T–: A549, $P = .048$; HCT-116, $P = .004$; MDA-MB-231, $P = .21$, log rank test) in each experimental group for the three cell lines. PAI-1 = plasminogen activator inhibitor-1; shRNA = short hairpin RNA; EFS = event-free survival.

More recent reports, however, suggested that PAI-1 may regulate tumor cell apoptosis and have a protumorigenic function. It was first reported that the addition of rPAI-1 to HL-60 and PC-3 tumor cells inhibits campothecin or etoposide-induced apoptosis (42). Overexpression of active PAI-1 in low PAI-1-expressing MDA-MB-435 breast cancer cells has also been shown to increase tumor cell survival upon paclitaxel treatment compared with cells expressing inactive PAI-1 (43), and mouse fibrosarcoma cells derived from PAI-1$^{-/-}$ mice were reported to be substantially more sensitive to etoposide-induced apoptosis than their counterparts derived from PAI-1$^{+/+}$ mice (44). The mechanism by which PAI-1 protects tumor cells from apoptosis is, however, not well understood. Fibrosarcoma cell lines derived from PAI-1$^{-/-}$ mice have an increased level of spontaneous apoptosis that is associated with a decreased activation of the PI3K/AKT cell survival pathway (31). In vascular smooth muscle cells, intracellular PAI-1 has also been reported to be antiapoptotic by direct inhibition of caspase-3, although the precise mechanism is unclear (45).

Here we provide evidence that endogenous PAI-1 protects tumor cells from apoptosis by a mechanism that is partially dependent on Fas/FasL-mediated apoptosis and the activation of plasmin by uPA. In support of uPA being an intermediate factor in the control of PAI-1 on apoptosis is the fact that we did not observe a direct correlation between the PAI-1 expression in tumor cells and the level of spontaneous apoptosis upon PAI-1 suppression (Figure 1). As the primary inhibitor of uPA, PAI-1 inhibits uPA-mediated plasminogen activation by promoting the rapid endocytosis of the trimolecular uPA/PAI-1/uPAR complex. Accordingly, we observed a statistically significant increase of uPA and subsequent increase in cell-associated plasmin activity upon PAI-1 downregulation in tumor cells in association with an increase in extrinsic apoptosis that could be in part prevented upon Fas and FasL blockade. As we found in EC, plasmin is involved in apoptosis in tumor cells, because the data indicate that complete plasmin inhibition by aprotinin in part reverses the apoptosis (Figure 3, C). These data thus indicate that the control of PAI-1

on tumor cell apoptosis is primarily indirect and dependent on uPA and plasmin activation, which is consistent with the fact that we observed similar levels of apoptosis in high PAI-1-expressing tumor cells (like HT-1080 cells) and low PAI-1-expressing cells (like HCT-116 cells). However, the absence of complete reversal of apoptosis in the presence of aprotinin (Figure 3, C) points to the possibility that PAI-1 may also have a plasmin-independent effect on tumor cell apoptosis. For example, PAI-1 may directly interact with other cell-associated receptors such as the low-density lipoprotein receptor–related protein 1 [LRP 1 (46)], which has been shown to protect neurons from apoptosis by activating an AKT-dependent survival pathway (47).

The fact that the addition of rPAI-1 could reverse the apoptosis induced by PAI-1 suppression in tumor cells points primarily to an extracellular effect of PAI-1 and suggests that paracrine PAI-1 produced within the tumor microenvironment may protect tumor cells lacking PAI-1 and vice-versa that PAI-1 produced by tumor cells may also protect normal cells like EC from apoptosis. This aspect was demonstrated in our xenotransplantation experiments that compared WT and PAI-1 KO mice. Among the four experimental groups of mice xenotransplanted with HT-1080, we only observed a statistically significant inhibition of tumorigenesis, a decrease in tumor take, and an increase in survival in group H–/T– mice in which PAI-1-deficient tumor cells were implanted in PAI-1 KO hosts. The analysis of the levels of human and murine PAI-1 in the murine plasma suggests that an inhibitory effect on tumorigenesis, as observed in group H–/T– mice, is only observed when PAI-1 plasma concentrations are at low levels (8.9; 95% CI = 2.6–15.1 ng/ml). PAI-1 levels in the plasma, however, only indirectly reflect what is occurring at the cell surface where PAI-1 controls the level of cell-associated plasm, and therefore from these data it may not be possible to conclude on the threshold level of PAI-1 needed to protect cells from apoptosis. In node-negative breast cancer patients in which PAI-1 was reported to be a predictor of poor prognosis, PAI-1 concentrations of at least 14 ng/ mg total protein in the primary tumor tissue were recently reported in patients with poor outcome (48). The absence of direct correlation between PAI-1 levels and apoptosis is consistent with an indirect effect of PAI-1 on apoptosis mediated in part by cell-associated plasmin.

The fact that PAI-1 suppression in both the host and the tumor (group H–/T–) substantially inhibited tumor uptake in HT-1080 and MDA-MB-231 models associated with the fact that human PAI-1 was always detected in the plasma of these mice when a tumor was developing (indicating a failure of the shRNA KD to completely suppress PAI-1 expression) should be emphasized. It suggests that in the total absence of PAI-1, tumor cells may stay dormant. Although the mechanism is not entirely understood at this point, it is conceivable that PAI-1 may be critical for the angiogenic switch necessary for tumors to develop. This possibility is consistent with the role of PAI-1 in protecting endothelial cells from apoptosis previously reported by us (28). In addition, an effect on cell adhesion, anoikis, and migration could also contribute (17,27).

The effect of genetic ablation of PAI-1 on tumor promotion and progression has been the subject of conflicting reports. Our data are consistent with previous reports showing that PAI-1 deficiency in mice markedly reduced tumor progression and angiogenesis in models of xenotransplantation (25,39). However, the effect of PAI-1 suppression in transgenic tumor models seems to be different. No effect on tumor development, primary tumor growth, angiogenesis, or lung metastasis was reported in PAI-1-deficient MMTV-PymT mice that develop spontaneous and metastatic mammary tumors (49). Similarly, no changes in tumor progression or angiogenesis were observed in PAI-1-deficient K14-HPV16 transgenic mice that develop spontaneous skin carcinoma (50). Interestingly, in PAI-1-deficient TRP-1/SV40 Tag mice that develop spontaneous metastatic ocular tumors derived from retinal pigmented epithelium, PAI-1 deficiency did not affect primary tumor growth or vascularization, but it was associated with a smaller number of brain metastases (51). The reason for this discrepancy is not completely understood, but the data may point to some important differences between transgenic and xenotransplanted models. In transgenic models of carcinogenesis, compensatory mechanisms for a lack of endogenous PAI-1 that could support tumor progression might be triggered during development. For example, an increased level of the angiogenic factor fibroblast growth factor-1 was found in the primary tumors of PAI-1-deficient TRP-1/SV40 Tag mice, and it may play a role in stimulating angiogenesis (51). Subtle differences between human and mouse PAI-1 may also play a role (52,53). In mice, PAI-1 activity in plasma is about fivefold lower than in humans, which points to the possibility that tumors from transgenic mice may be less dependent on PAI-1 for survival, whereas human tumors may require PAI-1 for survival and proliferation.

PAI-1 has been proposed as a target for therapeutic intervention in thrombotic diseases where elevated levels of PAI-1 represent a well-known risk factor and play a critical role in preventing the repermeabilization of a thrombus and in promoting restenosis (54–56). PAI-039 (Tiplaxtinin), a small molecule inhibitor of PAI-1 that is orally active, has been tested in several preclinical models of vascular thrombosis in rats and dogs and shown to be effective in inhibiting plasma PAI-1 and promoting thrombus repermeabilization (38,57,58). PAI-039 has also been shown to prevent the development of diet-induced obesity in a preclinical mouse model (59). There have been so far limited attempts to test the efficacy and safety of PAI-1 inhibitors in preclinical models of cancer. PAI-039 has been shown to inhibit EC motility and angiogenesis in Matrigel implants in mice (60). In this study, we provide data supporting an anticancer activity of PAI-039 by showing that it induces apoptosis in tumor cells at concentrations that inhibit PAI-1 activity in vitro (61). Because of the poor inhibitory activity of PAI-039 against vitronectin-bound PAI-1 (61), other PAI-1 inhibitors have been recently developed. For example, SK-216 and SK-116, two small molecular inhibitors of PAI-1, have been shown to reduce PAI-1 levels and suppress the formation of intestinal polyps in $Apc^{-/-}$ mice (62).

Our work also had some limitations. We examined the effect of PAI-1 suppression on spontaneous (unstimulated) apoptosis in tumor cells and not on apoptosis induced by stress. It would be interesting to determine whether PAI-1 has a similar protective effect on apoptosis induced by cytotoxic drugs or microenvironmental factors such as hypoxia. Second, this study pointed to the possibility of plasmin-independent mechanisms by which PAI-1 may protect tumor cells from spontaneous apoptosis. It is presently unknown whether such a mechanism involves a direct interaction between PAI-1 and cell-associated receptor-like LRP-1. Finally, in these

experiments, we used human cells xenotransplanted in immune-deficient mice and thus have not explored the potential contribution of the adaptive immune system on protumorigenic effect of PAI-1. These aspects are currently under investigation in our laboratory.

In conclusion, the data of this study suggest that similar to EC, PAI-1 exerts a protective effect against apoptosis in tumor cells by a mechanism that, in part, involves Fas/Fas-L-mediated apoptosis and plasmin activation and that both tumor- and host-derived PAI-1 play a role in tumor progression. These data also support PAI-1 as a therapeutic target in cancer and preclinical studies testing PAI-1 inhibitors in cancer therapy.

References

1. Werb Z. ECM and cell surface proteolysis: regulating cellular ecology. *Cell*. 1997;91(4):439–442.
2. Page-McCaw A, Ewald AJ, Werb Z. Matrix metalloproteinases and the regulation of tissue remodelling. *Nat Rev Mol Cell Biol*. 2007;8(3):221–233.
3. Overall CM, Blobel CP. In search of partners: linking extracellular proteases to substrates. *Nat Rev Mol Cell Biol*. 2007;8(3):245–257.
4. Blasi F, Sidenius N. The urokinase receptor: focused cell surface proteolysis, cell adhesion and signaling. *FEBS Lett*. 2010;584(9):1923–1930.
5. Dass K, Ahmad A, Azmi AS, Sarkar SH, Sarkar FH. Evolving role of uPA/uPAR system in human cancers. *Cancer Treat Rev*. 2008;34(2):122–136.
6. McMahon B, Kwaan HC. The plasminogen activator system and cancer. *Pathophysiol Haemost Thromb*. 2008;36(3–4):184–194.
7. Blasi F, Verde P. Urokinase-dependent cell surface proteolysis and cancer. *Semin Cancer Biol*. 1990;1(2):117–126.
8. Danø K, Behrendt N, Høyer-Hansen G, et al. Plasminogen activation and cancer. *Thromb Haemost*. 2005;93(4):676–681.
9. Duffy MJ, Duggan C, Mulcahy HE, McDermott EW, O'Higgins NJ. Urokinase plasminogen activator: a prognostic marker in breast cancer including patients with axillary node-negative disease. *Clin Chem*. 1998;44(6, pt 1):1177–1183.
10. de Witte JH, Foekens JA, Brünner N, et al. Prognostic impact of urokinase-type plasminogen activator receptor (uPAR) in cytosols and pellet extracts derived from primary breast tumours. *Br J Cancer*. 2001;85(1):85–92.
11. Ljuca D, Fatusić Z, Iljazović E, Ahmetović B. Monitoring of chemotherapy successfulness of platina/taxol chemotherapy protocol by using determination of serum urokinase plasminogen activator (uPA) and soluble urokinase plasminogen activator receptor (suPAR) in patients with ovarian carcinoma FIGO II and III stage. *Bosn J Basic Med Sci*. 2007;7(2):111–116.
12. Seddighzadeh M, Steineck G, Larsson P, et al. Expression of UPA and UPAR is associated with the clinical course of urinary bladder neoplasms. *Int J Cancer*. 2002;99(5):721–726.
13. Skelly MM, Troy A, Duffy MJ, et al. Urokinase-type plasminogen activator in colorectal cancer: relationship with clinicopathological features and patient outcome. *Clin Cancer Res*. 1997;3(10):1837–1840.
14. Dupont DM, Madsen JB, Kristensen T, et al. Biochemical properties of plasminogen activator inhibitor-1. *Front Biosci*. 2009;14:1337–1361.
15. Cale JM, Lawrence DA. Structure-function relationships of plasminogen activator inhibitor-1 and its potential as a therapeutic agent. *Curr Drug Targets*. 2007;8(9):971–981.
16. Bauman SJ, Whinna HC, Church FC. Serpins (serine protease inhibitors). *Curr Protoc Protein Sci*. 2002;Chapter 21:Unit 21.7.
17. Czekay RP, Aertgeerts K, Curriden SA, Loskutoff DJ. Plasminogen activator inhibitor-1 detaches cells from extracellular matrices by inactivating integrins. *J Cell Biol*. 2003;160(5):781–791.
18. Allgayer H, Heiss MM, Schildberg FW. Prognostic factors in gastric cancer. *Br J Surg*. 1997;84(12):1651–1664.
19. Berger DH. Plasmin/plasminogen system in colorectal cancer. *World J Surg*. 2002;26(7):767–771.
20. Foekens JA, Look MP, Peters HA, van Putten WL, Portengen H, Klijn JG. Urokinase-type plasminogen activator and its inhibitor PAI-1: predictors of poor response to tamoxifen therapy in recurrent breast cancer. *J Natl Cancer Inst*. 1995;87(10):751–756.
21. Harbeck N, Thomssen C, Berger U, et al. Invasion marker PAI-1 remains a strong prognostic factor after long-term follow-up both for primary breast cancer and following first relapse. *Breast Cancer Res Treat*. 1999;54(2):147–157.
22. Chambers SK, Ivins CM, Carcangiu ML. Plasminogen activator inhibitor-1 is an independent poor prognostic factor for survival in advanced stage epithelial ovarian cancer patients. *Int J Cancer*. 1998;79(5):449–454.
23. Kuhn W, Schmalfeldt B, Reuning U, et al. Prognostic significance of urokinase (uPA) and its inhibitor PAI-1 for survival in advanced ovarian carcinoma stage FIGO IIIc. *Br J Cancer*. 1999;79(11–12):1746–1751.
24. Zekanowska E, Cieslinski K, Rosc D. Plasminogen activator inhibitor type 1 (PAI-1) in blood and tissue extracts of patients with non-small cell lung cancer. *Pneumonol Alergol Pol*. 2004;72(9–10):409–414.
25. Bajou K, Noël A, Gerard RD, et al. Absence of host plasminogen activator inhibitor 1 prevents cancer invasion and vascularization. *Nat Med*. 1998;4(8):923–928.
26. Bajou K, Maillard C, Jost M, et al. Host-derived plasminogen activator inhibitor-1 (PAI-1) concentration is critical for in vivo tumoral angiogenesis and growth. *Oncogene*. 2004;23(41):6986–6990.
27. Isogai C, Laug WE, Shimada H, et al. Plasminogen activator inhibitor-1 promotes angiogenesis by stimulating endothelial cell migration toward fibronectin. *Cancer Res*. 2001;61(14):5587–5594.
28. Bajou K, Peng H, Laug WE, et al. Plasminogen activator inhibitor-1 protects endothelial cells from FasL-mediated apoptosis. *Cancer Cell*. 2008;14(4):324–334.
29. Madsen MA, Deryugina EI, Niessen S, Cravatt BF, Quigley JP. Activity-based protein profiling implicates urokinase activation as a key step in human fibrosarcoma intravasation. *J Biol Chem*. 2006;281(23):15997–16005.
30. Lademann UA, Rømer MU. Regulation of programmed cell death by plasminogen activator inhibitor type 1 (PAI-1). *Thromb Haemost*. 2008;100(6):1041–1046.
31. Rømer MU, Larsen L, Offenberg H, Brünner N, Lademann UA. Plasminogen activator inhibitor 1 protects fibrosarcoma cells from etoposide-induced apoptosis through activation of the PI3K/Akt cell survival pathway. *Neoplasia*. 2008;10(10):1083–1091.
32. Masters JR, Thomson JA, Daly-Burns B, et al. Short tandem repeat profiling provides an international reference standard for human cell lines. *Proc Natl Acad Sci U S A*. 2001;98(14):8012–8017.
33. Bekes EM, Deryugina EI, Kupriyanova TA, et al. Activation of pro-uPA is critical for initial escape from the primary tumor and hematogenous dissemination of human carcinoma cells. *Neoplasia*. 2011;13(9):806–821.
34. Sawaya R, Highsmith R. Plasminogen activator activity and molecular weight patterns in human brain tumors. *J Neurosurg*. 1988;68(1):73–79.
35. Carmeliet P, Kieckens L, Schoonjans L, et al. Plasminogen activator inhibitor-1 gene-deficient mice. I. Generation by homologous recombination and characterization. *J Clin Invest*. 1993;92(6):2746–2755.
36. Hoff J. Methods of blood collection in the mouse. *Lab Animal*. 2000;29(10):47–53.
37. Chantrain CF, DeClerck YA, Groshen S, McNamara G. Computerized quantification of tissue vascularization using high-resolution slide scanning of whole tumor sections. *J Histochem Cytochem*. 2003;51(2):151–158.
38. Elokdah H, Abou-Gharbia M, Hennan JK, et al. Tiplaxtinin, a novel, orally efficacious inhibitor of plasminogen activator inhibitor-1: design, synthesis, and preclinical characterization. *J Med Chem*. 2004;47(14):3491–3494.
39. Gutierrez LS, Schulman A, Brito-Robinson T, Noria F, Ploplis VA, Castellino FJ. Tumor development is retarded in mice lacking the gene for urokinase-type plasminogen activator or its inhibitor, plasminogen activator inhibitor-1. *Cancer Res*. 2000;60(20):5839–5847.
40. Devy L, Blacher S, Grignet-Debrus C, et al. The pro- or antiangiogenic effect of plasminogen activator inhibitor 1 is dose dependent. *FASEB J*. 2002;16(2):147–154.
41. Cajot JF, Bamat J, Bergonzelli GE, et al. Plasminogen-activator inhibitor type 1 is a potent natural inhibitor of extracellular matrix degradation by fibrosarcoma and colon carcinoma cells. *Proc Natl Acad Sci U S A*. 1990;87(18):6939–6943.
42. Kwaan HC, Wang J, Svoboda K, Declerck PJ. Plasminogen activator inhibitor 1 may promote tumour growth through inhibition of apoptosis. *Br J Cancer*. 2000;82(10):1702–1708.

43. Beaulieu LM, Whitley BR, Wiesner TF, et al. Breast cancer and metabolic syndrome linked through the plasminogen activator inhibitor-1 cycle. *Bioessays*. 2007;29(10):1029–1038.
44. Rømer MU, Kirkebjerg Due A, Knud Larsen J, et al. Indication of a role of plasminogen activator inhibitor type I in protecting murine fibrosarcoma cells against apoptosis. *Thromb Haemost*. 2005;94(4):859–866.
45. Chen Y, Kelm RJ Jr, Budd RC, Sobel BE, Schneider DJ. Inhibition of apoptosis and caspase-3 in vascular smooth muscle cells by plasminogen activator inhibitor type-1. *J Cell Biochem*. 2004;92(1):178–188.
46. Degryse B, Neels JG, Czekay RP, Aertgeerts K, Kamikubo Y, Loskutoff DJ. The low density lipoprotein receptor-related protein is a motogenic receptor for plasminogen activator inhibitor-1. *J Biol Chem*. 2004;279(21):22595–22604.
47. Fuentealba RA, Liu Q, Kanekiyo T, Zhang J, Bu G. Low density lipoprotein receptor-related protein 1 promotes anti-apoptotic signaling in neurons by activating Akt survival pathway. *J Biol Chem*. 2009;284(49):34045–34053.
48. Kantelhardt EJ, Vetter M, Schmidt M, et al. Prospective evaluation of prognostic factors uPA/PAI-1 in node-negative breast cancer: phase III NNBC3-Europe trial (AGO, GBG, EORTC-PBG) comparing 6×FEC versus 3×FEC/3×Docetaxel. *BMC Cancer*. 2011;11:140.
49. Almholt K, Nielsen BS, Frandsen TL, Brünner N, Danø K, Johnsen M. Metastasis of transgenic breast cancer in plasminogen activator inhibitor-1 gene-deficient mice. *Oncogene*. 2003;22(28):4389–4397.
50. Masset A, Maillard C, Sounni NE, et al. Unimpeded skin carcinogenesis in K14-HPV16 transgenic mice deficient for plasminogen activator inhibitor. *Int J Cancer*. 2011;128(2):283–293.
51. Maillard CM, Bouquet C, Petitjean MM, et al. Reduction of brain metastases in plasminogen activator inhibitor-1-deficient mice with transgenic ocular tumors. *Carcinogenesis*. 2008;29(11):2236–2242.
52. Declerck PJ, Gils A, De Taeye B. Use of mouse models to study plasminogen activator inhibitor-1. *Meth Enzymol*. 2011;499:77–104.
53. Matsuo O, Lijnen HR, Ueshima S, Kojima S, Smyth SS. A guide to murine fibrinolytic factor structure, function, assays, and genetic alterations. *J Thromb Haemost*. 2007;5(4):680–689.
54. Meltzer ME, Doggen CJ, de Groot PG, Rosendaal FR, Lisman T. The impact of the fibrinolytic system on the risk of venous and arterial thrombosis. *Semin Thromb Hemost*. 2009;35(5):468–477.
55. Brown NJ. Therapeutic potential of plasminogen activator inhibitor-1 inhibitors. *Ther Adv Cardiovasc Dis*. 2010;4(5):315–324.
56. Lijnen HR. Role of fibrinolysis in obesity and thrombosis. *Thromb Res*. 2009;123(suppl 4):S46–S49.
57. Hennan JK, Morgan GA, Swillo RE, et al. Effect of tiplaxtinin (PAI-039), an orally bioavailable PAI-1 antagonist, in a rat model of thrombosis. *J Thromb Haemost*. 2008;6(9):1558–1564.
58. Hennan JK, Elokdah H, Leal M, et al. Evaluation of PAI-039 [{1-benzyl-5-[4-(trifluoromethoxy)phenyl]-1H-indol-3-yl}(oxo)acetic acid], a novel plasminogen activator inhibitor-1 inhibitor, in a canine model of coronary artery thrombosis. *J Pharmacol Exp Ther*. 2005;314(2):710–716.
59. Crandall DL, Quinet EM, El Ayachi S, et al. Modulation of adipose tissue development by pharmacological inhibition of PAI-1. *Arterioscler Thromb Vasc Biol*. 2006;26(10):2209–2215.
60. Leik CE, Su EJ, Nambi P, Crandall DL, Lawrence DA. Effect of pharmacologic plasminogen activator inhibitor-1 inhibition on cell motility and tumor angiogenesis. *J Thromb Haemost*. 2006;4(12):2710–2715.
61. Gorlatova NV, Cale JM, Elokdah H, et al. Mechanism of inactivation of plasminogen activator inhibitor-1 by a small molecule inhibitor. *J Biol Chem*. 2007;282(12):9288–9296.
62. Mutoh M, Niho N, Komiya M, et al. Plasminogen activator inhibitor-1 (Pai-1) blockers suppress intestinal polyp formation in Min mice. *Carcinogenesis*. 2008;29(4):824–829.

Funding

National Cancer Institute (grant CA129377 to YAD, VPR). HF was supported by a pre-doctoral Award from The Saban Research Institute of Children's Hospital Los Angeles.

Notes

The authors thank Ms Jackie Tsen-Yin Lin, Dr Fred Dorey, and Dr G. Esteban Fernandez for their excellent technical support and Ms J. Rosenberg for her typing and editing of the manuscript. H. Fang contributed to the design of the study, performed most of the experiments, generated and interpreted the data, and wrote the manuscript. V. R. Placencio contributed to the data described under Figures 1 and 5 and helped in the reviewing and editing of the manuscript. Y. A. DeClerck generated the concept, contributed to the design, supervised the performance of the experiments and the data analysis, and critically reviewed and edited the manuscript and contributed to the writing.

Affiliations of authors: Division of Hematology-Oncology, Department of Pediatrics (HF, VRP, YAD), Department of Pathology (HF), and Department of Biochemistry and Molecular Biology (YAD), Keck School of Medicine, University of Southern California, Los Angeles, CA; Cancer Program, The Saban Research Institute of Children's Hospital Los Angeles (HF, VRP, YAD), Los Angeles, CA.